Role of adipose tissue in the host immune response to *Neospora caninum* infection

Joana Teixeira Pinto de Melo
Mestrado em Bioquímica
Departamento de Química e Bioquímica
2013

Orientador
Doutora Luzia Teixeira, Investigador Auxiliar, ICBAS-UP

Coorientadores
Professor Doutor Manuel Vilanova, Professor Associado, ICBAS-UP
Professora Doutora Paula Ferreira, Professor Associado, ICBAS-UP

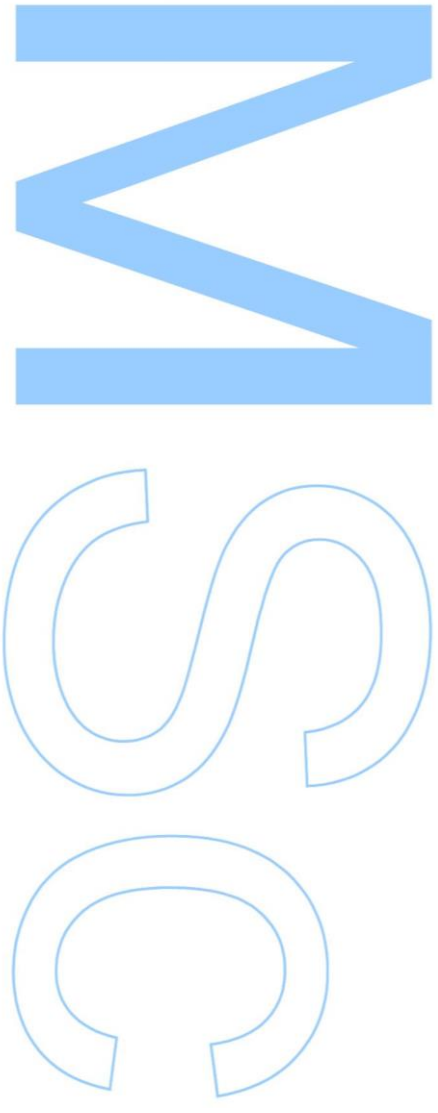

U.PORTO

FACULDADE DE CIÊNCIAS
UNIVERSIDADE DO PORTO

INSTITUTO DE CIÊNCIAS BIOMÉDICAS ABEL SALAZAR
UNIVERSIDADE DO PORTO

Todas as correções determinadas pelo júri, e só essas, foram efetuadas.
O Presidente do Júri,

Porto, _____/_____/_____

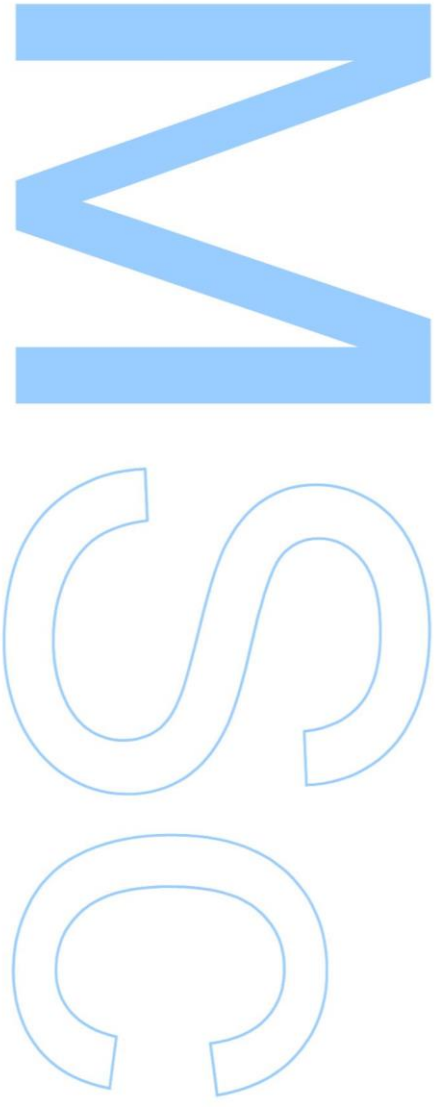

Part of this work was presented at the XXXIX Annual Meeting of the Portuguese Society of Immunology has a poster communication, in 13-15 November 2013:

Joana Melo, Sofia Jesus, João Moreira, Raquel M. Marques, Pedro Ferreirinha, Alexandra Correia, Filipa Bezerra, Ana Pinto, Madalena Costa, Paula G. Ferreira, Manuel Vilanova, Artur P. Águas, Luzia Teixeira. “Macrophages and regulatory T cells accumulate in the adipose tissue of mice infected with *Neospora caninum*”.

Acknowledgements

First of all, I would like to thank my supervisor Luzia Teixeira for the opportunity to work with her. Her guidance and knowledge was fundamental for my work and development as a lab professional.

I am thankful to my co-supervisors Professor Manuel Vilanova and Professor Paula Ferreira, whose encouragement, knowledge and support was fundamental to finish my master's thesis.

I am grateful to the whole Departamento de Anatomia of Instituto de Ciências Biomédicas Abel Salazar, for having welcomed me so well. To Professor Artur Águas, for allowing me the opportunity to develop my thesis in his laboratory. To Raquel, Madalena, Ana, Sofia P. and Tiago, for all the help, laughs, talks, distractions and, above all, the companionship. To Sr. Duarte, Sr. Costa, D. Manuela and Gil, for all the spoiling, the joyful "good-mornings", the cadaverous views and the bantering moments.

To Alexandra, Pedro Ferreirinha and Begoña, for the constant guidance, support and availability. In particular, to Pedro and Begoña for all the help with the animal handling.

I am thankful to Fátima Ferreirinha for her endless help, patience and time spent on confocal microscopy imaging.

To Sofia, for enduring my moods, complaints throughout the year and for all the help given. To Romeu and Joana, for all the funny moments.

To all my friends, a big thank you! In special to Rita, Viais, Nilma, Escuteiro, Diogo, Ricardo e Ju. You have handled the worst of me when I was stressed out, but had the best of me when I was happy and excited. Each of you helped me in your own special way, no matter how far or how often we saw each other. Without you all, I could not go through this year alive!

Ângela, thanks for the talks, tears, laughs. Your support and company have both been essential for me.

I want to thank Zé for the laughs and funny moments you have granted to me with that way of yours. Despite our disagreements, never doubt you are very special to me! <3

Por último, mas não menos importante, queria agradecer aos meus pais e à minha família todo o apoio e confiança que depositaram em mim. Sem vocês, eu não teria as oportunidades que tenho tido e não seria a pessoa que sou. Tenho o maior orgulho em todos vocês! Em particular à minha mãe, ao meu pai e à minha tia, um muito obrigado! À Eduarda, obrigada pelo carinho! Um obrigado especial à Clarinha, pelo miminho e por cada abraço, capazes de fazer desaparecer todos os problemas.

This work is supported by FEDER through COMPETE and by national funds through FCT - FCOMP-01-0124-FEDER-020158 (FCT reference: PTDC/CTV/122777/2010).

Abstract

The intracellular protozoan *Neospora caninum* is a major pathogen of canids and cattle. Neosporosis, is an important cause of abortion in cows thus causing severe economic losses in dairy and beef industry. The study of the protective immune response triggered by the host against *N. caninum* is therefore of utmost importance towards the development of an effective vaccine against this parasitosis.

It has been described that adipose tissue is a reservoir for some microorganisms, including protozoan parasites, with functions beyond the mere accumulation of triglycerides and maintenance of energy homeostasis, as it may also contribute to host immunity. Taking this into account, this work aims at providing a first approach to elucidate the role of adipose tissue in the host immune response to *N. caninum* infection.

Wild-type C57BL/6 mice, were inoculated by the intraperitoneal route with *N. caninum* tachyzoites and 6 hours, 7 days and 2 months after challenge, subcutaneous, intramuscular and visceral (omental, gonadal and mesenteric) adipose tissue samples were collected. Even though *N. caninum* tachyzoites were detected by immunohistochemistry 6 hours after infection in the visceral adipose tissue, only parasitic DNA could be detected therein by 7 days of infection and no parasitic DNA was detected by 2 months of infection. This indicates that adipose tissue is not a reservoir for *N. caninum* in the host.

The study of immune cell populations in the adipose tissue, at 7 days of infection, revealed a local increase in $F4/80^+$ and $Foxp3^+$ cells in the infected mice, as assessed either by immunohistochemistry or flow cytometry. An increase in $NK1.1^+$, $TCR\gamma\delta^+$, $TCR\beta^+NK1.1^+$, $CD4^+$ and $CD8^+$ T cell numbers was also observed in the adipose tissue depots of infected mice by flow cytometric analysis. The production of IFN-γ was assessed in these five populations, which were all found to be IFN-γ-producers upon the parasitic challenge. IFN-γ and IL-10 double producers were detected among $CD4^+$ and $CD8^+$ T cells upon infection.

Altogether, the findings reported here show that the adipose tissue contributes for the host immune response in mice intraperitoneally challenged with *N. caninum* tachyzoites.

Keywords: *Neospora caninum*, adipose tissue, macrophages, Treg cells, IFN-γ

Resumo

O protozoário intracelular *Neospora caninum* é um agente patogénico que infeta canídeos e gado bovino. A neosporose é uma importante causa de aborto em bovinos, levando a perdas económicas significativas na indústria leiteira e de produção de carne. O estudo da resposta imunitária protetora desencadeada pelo hospedeiro contra *N. caninum* tem portanto elevada importância para o desenvolvimento de uma vacina eficaz contra este parasita.

Já foi descrito que o tecido adiposo serve de reservatório para alguns microorganismos, incluindo protozoários, apresentando funções não só de reserva de triglicéridos e manutenção da homeostasia energética, contribuindo também para a imunidade do hospedeiro. Assim, este trabalho representa uma primeira abordagem ao papel do tecido adiposo na resposta imunitária de ratinhos à infeção com *N. caninum*.

Ratinhos C57BL/6 *wild-type* foram inoculados pela via intraperitoneal com taquizoítos de *N. caninum* e 6 horas, 7 dias e 2 meses após a injeção foram recolhidas amostras de tecido adiposo subcutâneo, intramuscular e visceral (omental, gonadal e mesentérico). Apesar de se terem detetado taquizoítos no tecido adiposo visceral, por imunohistoquímica, 6 horas após a infecção, apenas se detetou DNA do parasita aos 7 dias de infeção, o que não se verificou após 2 meses de infeção. Este resultado indica que o tecido adiposo não é um reservatório para *N. caninum* no hospedeiro.

O estudo das populações celulares do sistema imunitário existentes no tecido adiposo, por imunohistoquímica e citometria de fluxo, revelou um aumento local das células F4/80$^+$ e Foxp3$^+$ em amostras de ratinhos infetados, ao sétimo dia após a infeção. A análise por citometria de fluxo também revelou um aumento no número das células NK1.1$^+$, TCRγδ$^+$, TCRβ$^+$NK1.1$^+$, T CD4$^+$ e T CD8$^+$ nos diferentes tipos de tecido adiposo de ratinhos infetados. Em todas estas populações foi detetada a presença de células produtoras de IFN-γ. Foram também observadas células T CD4$^+$ e T CD8$^+$ duplas produtoras de IFN-γ e IL-10.

Os nossos resultados sugerem que o tecido adiposo contribui para a resposta imunitária desenvolvida pelo hospedeiro em ratinhos infetados pela via intraperitoneal com taquizoítos de *N. caninum*.

Palavras-chave: *Neospora caninum*, tecido adiposo, macrófagos, células T reguladoras, IFN-γ

Table of contents

List of figures

List of tables

Abbreviations

ABC	Avidin/Biotin complex
APC	Antigen-presenting cells
BAT	Brown adipose tissue
BSA	Bovine serum albumin
CLS	Crown-like structures
CNS	Central nervous system
DAB	3,3'-diaminobenzidine
DC	Dendritic cells
ELISA	Enzyme-Linked Immunosorbent Assay
FALC	Fat-associated lymphoid clusters
FBS	Fetal bovine serum
FVD	Fixable viability dye
H_2O_2	Hydrogen peroxide
IFAT	Indirect Fluorescent Antibody Test
IFN	Interferon
IL	Interleukin
IL-1Ra	IL-1 receptor antagonist
Ig	Immunoglobulin
i.g.	Intragastric
IHC	Immunohistochemistry
IMAT	Intramuscular adipose tissue
iNKT	Invariant natural killer T cells
i.p.	Intraperitoneal
LPS	Lipopolysaccharide
mAbs	Monoclonal antibodies
MEM	Minimum essential medium
MHC	Major Histocompatibility Complex
MHV68	Murine gammaherpesvirus 68
MLN	Mesenteric lymph nodes
NAT	*Neospora* Agglutination Test
NcDG1	*Neospora caninum* dense granule protein 1
NcSAG1	*Neospora caninum* surface antigen 1
NcSRS2	*Neospora caninum* surface antigen related sequence 2
NcT	*Neospora caninum* tachyzoites

NK	Natural killer
NO	Nitric oxide
PBS	Phosphate-buffered saline
PCR	Polymerase Chain Reaction
RT-PCR	Real-time Polymerase Chain Reaction
p.i.	Post infection
PMA	Phorbol 12-myristate 13-acetate
RT	Room temperature
SAT	Subcutaneous adipose tissue
SVF	Stromal vascular fraction
TBS	Tris-buffered saline
TCR	T cell receptor
Treg	Regulatory T cell
VAT	Visceral adipose tissue
WAT	White adipose tissue
WT	Wild-type

Introduction

1. *Neospora caninum*

1.1. Biology of *Neospora caninum*

Neospora caninum is an obligate intracellular protozoan parasite closely related to *Toxoplasma gondii* that was first described in 1984 by Bjerkas *et al* as a causative agent of lesions in the central nervous system (CNS) and skeletal muscles in dogs [1]. Later, Parish *et al* and O'Toole and Jeffrey also associated this parasite with myeloencephalitis in calves [2, 3]. However, the isolation and description of this parasite was only accomplished in 1988 by Dubey *et al* [4], which proposed a new genus *Neospora* and a new specie *Neospora caninum*, belonging to the family *Sarcocystidae* and phylum Apicomplexa.

N. caninum has been isolated from diverse animal hosts. Dog (*Canis domesticus*), coyote (*Canis latrans*) and gray wolf (*Canis lupus*) are confirmed definitive hosts while cattle, sheep, water buffalo, horse, bison and deer represent some of the identified intermediate hosts [5, 6].

At present, there are no reported evidences indicating that this parasite successfully infects humans [7]. However, the experimental inoculation of monkeys with *N. caninum*, which resulted in transplacental transmission and foetal infection [8], and the detection of *N. caninum*-specific immunoglobulin (Ig) G in the sera of HIV-infected patients or patients with neurological disorders [9] raised some concerns in this regard.

1.2. Life Cycle

The life cycle of *N. caninum* encompasses three known infectious stages: tachyzoites, bradyzoites and oocysts, and has two distinct modes of reproduction: sexual reproduction, which takes place in the definitive host, and asexual reproduction, in intermediate hosts [10, 11].

The tachyzoites, with an ovoid, lunate or globular shape, measure approximately 6×2 μm and invade and infect different cell types of the intermediate hosts. When within the host cell cytoplasm, in a parasitophorous vacuole, they rapidly replicate by endodyogeny and differentiate into bradyzoites that form cysts in tissues [10, 12, 13]. The bradyzoites are elongate, measuring aproximately 8×2 μm and slowly replicate by endodyogeny. The tissue cysts, round or oval in shape, are found in neural or skeletal muscle cells and persist on the intermediate host without causing clinical manifestations [10, 12, 14, 15]. The tachyzoites and the bradyzoites therefore represent the asexual

stage of *N. caninum* [10]. The oocyst, the sexual infectious stage, is excreted in the faeces of the definitive host in an unsporulated stage and represents the resistant stage on the environment [16]. Outside the host, oocysts sporulate in 24 to 72 hours, to form two sporocysts, containing four sporozoites each [10, 17, 18].

It is believed that infection of the definitive hosts occurs after ingestion of raw meat that contains the encysted stage of *N. caninum* (Figure 1) [18]. On the gut, bradyzoites are released and infect epithelial cells of the small intestine, a stage that precedes the formation of oocysts. The infected hosts excrete unsporulated oocysts in the feces that could contaminate pasture or water and may be ingested by intermediate hosts. After ingestion of sporulated oocysts, sporozoites are thought to be released in the intestinal tract, invading the host cells and becoming tachyzoites, which will divide and quickly spread to other cell types throughout the host before they differentiate into bradyzoites that will form tissue cysts. One of the factors that cause the conversion to this slowly proliferating stage is believed to be the stress during the host immune response against the parasite, being the tissue cysts a way of protection. This stage remains latent until the host immune system is suppressed, which probably allows them to recrudesce. The life cycle is complete when tissue cysts are ingested by a definitive host [10, 11, 17, 19].

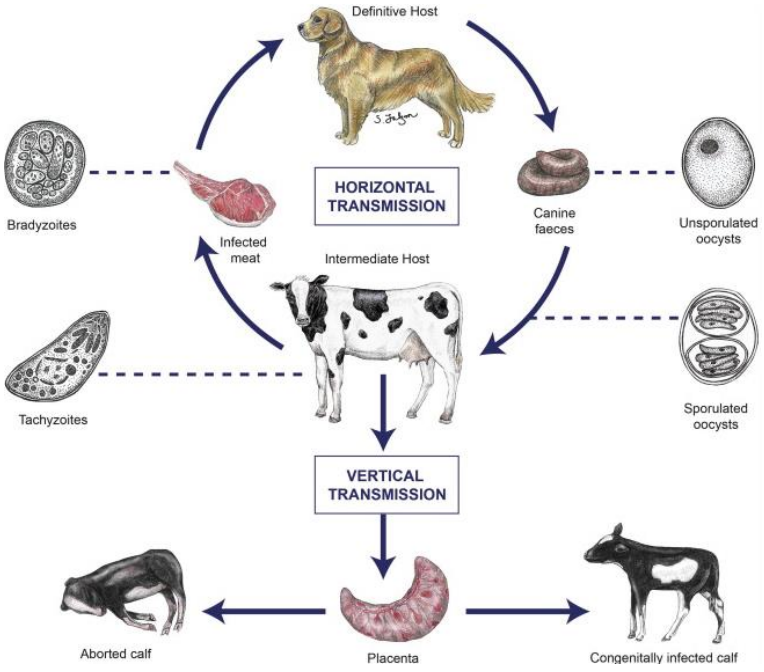

Figure 1. Life cycle of *Neospora caninum* [10].

The mode of transmission of *N. caninum* can be the one described before and is referred to postnatal, or horizontal, or can occur from infected mother to foetus during pregnancy and is referred to transplacental, or vertical (Figure 1). Both routes of transmission play an important role in infection and are vital for the survival of the parasite

[20]. The principal route of infection in cattle, the major intermediate host, is vertical transmission and can occur in postnatally acquired infections by ingestion of oocysts by the mother or by reactivation of infection in a chronically infected cow [10, 11, 17].

1.3. Neosporosis

Infection by *N. caninum* leads to neosporosis, a disease causative of abortion, stillbirth, neurologic signs and maternal infertility in cattle, which may lead to death, in various affected animals [12, 21].

In dogs, the most severe cases of neosporosis occur in young and congenitally infected pups, which develop hind limb paresis, leading to progressive paralysis, difficulty in swallowing, muscle flaccidity, muscle atrophy and heart failure [12].

In cattle, abortion is the main clinical manifestation of this disease. Fetuses may die *in utero* or be reabsorbed, mummified, autolyzed, stillborn, born alive with clinical signs or born clinically normal but persistently infected. Adult cattle infected with the parasite do not exhibit clinical signs of the disease, but the type of manifestation in calves is dependent on whether the mother is pregnant or not at the time of infection and on the phase of gestation when they become infected [10, 17, 22].

As an important cause of abortion in cattle, bovine neosporosis is a disease of worldwide concern, representing reproductive losses, early foetal death, reduction in milk production and premature culling [23].

1.4. Diagnosis Methods

In aborted foetuses or other hosts, the detection of *N. caninum* is accomplished by histologic examination of lesions followed by immunohistochemical staining of tissue sections using antibodies specific for the parasite. However, immunohistochemistry (IHC) is a low sensitivity technique, being polymerase chain reaction (PCR) detection and quantification of parasitic DNA a more sensible method for the diagnosis of neosporosis [11, 24].

In order to detect *N. caninum* antibodies, several serologic tests can be used, such as Enzyme-Linked Immunosorbent Assay (ELISA), Indirect Fluorescent Antibody Test (IFAT) and *Neospora* Agglutination Test (NAT). They are performed on sera, plasma or milk samples and provide information at which stage of infection the animal is. However, the results may not be straightforward because the antibody levels change during the course of the infection, according to the infectious stage of the parasite [17, 24].

2. Immunity to *Neospora caninum*

2.1. Innate immune response

The cellular populations responsible for the protective innate immune response against *N. caninum* all share the feature of producing or stimulate the production of interferon-γ (IFN-γ).

Natural Killer (NK) cells are important in early innate immune responses and play an essential role in host resistance against protozoan infections [25]. *In vitro* studies have demonstrated the capacity of bovine NK cells to produce IFN-γ after the exposure to *N. caninum*-infected fibroblasts, a response independent of interleukin IL-12, but potentiated in the presence of this cytokine [26]. Klevar *et al* also demonstrated the contribution of NK cells to IFN-γ production in the early stages of *N. caninum* infection, by *in vivo* studies [27].

Likewise, macrophages have a crucial role in protective immunity against parasite infection. A major function of macrophages is their killing activity against this intracellular parasite associated with increased production of nitric oxide (NO), which is IFN-γ-dependent [28, 29].

Dendritic cells (DC) are the major antigen-presenting cells (APC), presenting the ability to mediate the innate immune response and regulate the adaptive immunity. Teixeira *et al* reported that, upon *N. caninum* intraperitoneal (i.p.) infection, splenic DC from BALB/c mice showed upregulation of surface costimulatory (CD40, CD80 and CD86) and major histocompatibility complex (MHC) class II molecules and were also identified as early sources of IL-12 [30]. Recently, Correia *et al* confirmed DC as early IL-12-producers, on mesenteric lymph nodes (MLN), upon intragastric (i.g.) challenge of C57BL/6 mice [31].

2.2. Cellular immune response

The type of immune response generated following infection determines protective immunity, being the resistance to neosporosis associated with IFN-γ and IL-12 production, a type 1 T (Th1) immune response, and susceptibility to this infection associated with IL-4 production, a Th2 response [32-35]. In C57BL/6 mice, challenged i.g. with *N. caninum* tachyzoites (NcT), it was detected an early IFN-γ production by $TCR\alpha\beta^{+}CD8^{+}$ T cells in the intestinal epithelium, MLN and spleen and later by $TCR\alpha\beta^{+}CD4^{+}$ T cells in the spleen and MLN [31]. Tanaka *et al* have proved a major role of $CD4^{+}$ T cells in response to *N. caninum* infection as compared with $CD8^{+}$ T cells by showing that BALB/c mice depleted of $CD4^{+}$ T cells succumbed to infection earlier than mice depleted of $CD8^{+}$ T cells [35].

Later, it was described that the number of $CD4^+$ T cells gradually increased upon infection in WT mice, but not in IFN-γ-deficient mice [29].

The importance of specific cytokines, namely IL-12 and IFN-γ, and their central role in resistance to acute neosporosis was observed *in vivo*. IFN-γ or IL-12-depleted mice with specific monoclonal antibodies exhibited advanced morbidity and rendered susceptible to parasite infection [32, 33, 35]. The importance of IFN-γ was demonstrated in IFN-γ-deficient mice that died within 9 days after *N. caninum* infection, where treatment of these mice with exogenous IFN-γ extended their lives [29]. Moreover, Botelho *et al* have shown the high susceptibility of C57BL/10ScCr mice to *N. caninum* infection. These mice, which do not express a functional IL-12 receptor, as well as toll-like receptor 4, have an impaired IFN-γ production upon *N. caninum* infection that was associated with their high susceptibility to this parasite [36].

The bias towards a Th1 or Th2 response in the course of *N. caninum* infection could be evaluated by assessing the levels of IL-4. The IFN-γ:IL-4 ratio thus reflects the type of immune response occurring during infection. Long *et al* verified that B10.D2 mice, a strain resistant to encephalitis, presented a high IFN-γ:IL-4 ratio and C57BL/6 and BALB/c mice, susceptible strains, presented a low IFN-γ:IL-4 ratio [34]. Later, Baszler *et al* confirmed the association of a low IFN-γ:IL-4 ratio and the consequent severe clinical manifestations associated with chronic infection on infected BALB/c mice [37].

Another cytokine produced during *N. caninum* infection is IL-10, which possesses immunosuppressive properties and has been associated to susceptibility to neosporosis. Splenocytes from infected IL-12-depleted mice showed an increase in mRNA expression for IL-10, 7 days post infection (p.i.), possible responsible for the observed lack of inflammation in the infected foci [33].

Immunosuppressive regulatory T (Treg) cells are characterized by expression of the forkhead box P3 transcription factor, Foxp3 [38]. In a *Trypanosoma cruzi* infection model, it was described an immunosuppressive activity of $CD4^+CD25^+$ Treg cells, allowing parasite proliferation and the development of an acute infection [39]. In a *N. caninum* infection, Treg cells may contribute to the establishment of a chronic infection, once it was demonstrated in *in vitro* study a suppressive activity of splenic and MLN $CD4^+CD25^+$ T cells sorted from i.g.-infected C57BL/6 mice [31].

2.3. Humoral immune response

In mice, Th1 cytokines favour the production of IgG2a antibodies and Th2 cytokines are associated with IgG1 antibody production [40]. An increased IgG1:IgG2a ratio was observed after immunization of BALB/c mice with a soluble antigen derived from

N. caninum tachyzoites, which enhanced brain lesions [37]. Baszler *et al* studied the IgG1 and IgG2a antibody titers after IFN-γ depletion or IL-12 administration in BALB/c mice. Consistent with a Th2-type immune response, IFN-γ depletion increased the IgG1:IgG2a ratio. On the contrary, IL-12 administration established a Th1 immune response with a lower IgG1:IgG2a ratio, at 3 weeks p.i., evolving to a mixed Th1/Th2 immune response at 6 weeks p.i. [32].

The presence of *N. caninum*-specific IgA was previously assessed in BALB/c mice infected by the i.p. or i.g. route and was only detected in the intestinal lavage fluids of i.g. challenged mice, showing that a specific humoral immune response could be elicited in the intestinal mucosa [41].

3. Vaccination strategies

The economic importance of neosporosis, especially in cattle, has led to research on the development of an effective vaccine or other means for prevention of *N. caninum* infection and vertical transmission. An optimal vaccine should stimulate protective cellular immune responses as well as a humoral immune response at both mucosal and systemical level, and is expected to include a combination of *N. caninum* antigens [42, 43].

There are several studies using different types of vaccines: live-attenuated, killed, containing *N. caninum* surface antigens or vector vaccines. Live vaccines are attenuated in one or more of their phenotypic characteristics and are successful at inducing appropriate immunity [43, 44]. Williams *et al* reported protection against experimental *N. caninum* infection in cattle during pregnancy using a naturally attenuated parasite isolate, followed by a strong cellular immune response and IFN-γ production [45]. However, live vaccines present several disadvantages such as the possibility of reversal to virulence, a short shelf-life and high cost. On the contrary, the use of killed parasite lysate in a vaccine is considered safer, but unable to stimulate the required cellular immune response. This type of vaccine may also contain nonprotective or immunosuppressive antigens or induce undesired responses [43, 44].

In order to overcome the disadvantages of live and killed vaccines, there is the need of developing a vaccine that includes a combination of *N. caninum* antigens which will induce an effective immune response [43]. Examples of these antigens are parasite surface proteins and proteins of secretory organelles, such as micronemes, rhoptries and dense granules [42]. A study performed by Cho *et al* indicated that a combined vaccine with *Neospora caninum* surface antigen related sequence 2 (NcSRS2) and *Neospora caninum* dense granule protein 1 (NcDG1) induced protective effect against *N. caninum*

infection [46]. Also, the immunization of BALB/c mice with recombinant NcSRS2 iscoms (immunostimulating complexes) induced specific antibodies to native NcSRS2 and a significant reduction of cerebral parasite load in immunized mice [47]. Nishikawa *et al* reported the use of a recombinant vaccinia virus to deliver NcSRS2 and *Neospora caninum* surface antigen 1 (NcSAG1) to BALB/c mice, which induced the production of IgG1 antibodies and IFN-γ and also provided effective protection against vertical transmission [48, 49].

At the moment, there is no effective vaccine available to control neosporosis. The only commercialized *N. caninum* vaccine, Neoguard™, composed of inactivated tachyzoites, has been taken off the market due to ambiguous efficacy [50, 51].

4. Adipose tissue

4.1. Adipose tissue biology

Adipose tissue is a specialized connective tissue extensively laden with adipocytes, but also composed of various other cell types. Adipocytes secrete a wide variety of hormones and proteins, commonly referred to as adipokines, which regulate whole body homeostasis [52]. Mammals have two main types of adipose tissue, white adipose tissue (WAT) and brown adipose tissue (BAT), each of which possesses unique functions. While WAT is increasingly recognized for its function in the regulation of energy metabolism, its contribution to some aspects of the immune system and as a site for energy storage, BAT is the main tissue regulating thermogenesis [53, 54].

WAT is primarily composed of tightly packed spherical adipocytes with unilocular lipid droplet, ranging from 30-130 μm in diameter, supported by a richly vascularized loose connective tissue [54]. The non-adipocyte component of this tissue is called the stromal vascular fraction (SVF), which comprises multipotent stem cells, pre-adipocytes, fibroblasts, endothelial cells of vessels and immune cells. Body distribution of WAT may be divided primarily into subcutaneous (SAT), adipose tissue present under the skin, and visceral (VAT) fat, adipose tissue that surrounds inner organs [54, 55]. However, when the quantity of nutrients exceeds the adipose tissue capacity, the overload is transferred into organs such as the liver, pancreas or to skeletal muscles. In skeletal muscles in particular, fat depots are located within perimysial connective tissue alongside myofibers and called intramuscular adipose tissue (IMAT). VAT may be further divided into several fat depots, such as omental, mesenteric and gonadal [54, 56].

There is an anatomical association between adipose tissue and lymphoid cells since some adipocytes surround lymph nodes and function as a source of fatty acids [57]. However, lymphoid cells are in intimate contact with adipocytes in other anatomical

locations, where there are no lymph nodes [55]. It is known that immune cells within adipose tissue and the inflammatory cytokines produced by them can significantly alter adipose tissue metabolism and endocrine function [58].

4.2. Lymphoid structures

Omental VAT, also called omentum, is a fatty tissue that connects the spleen, stomach, pancreas and colon and is enriched in macrophages, B-1 B cells, DC and NK T cells. These leukocytes are organized into clusters termed milky spots that collect fluids, bacteria and cells from the peritoneal cavity and might induce an immune response. Milky spots increase in size and number in response to the presence of bacteria in the peritoneal cavity. Although B-1 B cells predominate in this structure and are important to confer immunity to bacterial pathogens, conventional (B-2) B cells responses can be identified as well, providing systemic humoral immunity [59, 60].

Lymphoid clusters have also been identified in mesenteric and gonadal VAT and are named fat-associated lymphoid clusters (FALC). FALC cells express multiple Th2 cytokines, mainly IL-4, IL-5, IL-6 and IL-13 [59].

4.3. Innate immunity

Innate immune cells, including macrophages, DC, neutrophils, mast cells and eosinophils, have been identified in adipose tissue, where macrophages are the majority of the present APC [61].

Macrophages in adipose tissue have been implicated in angiogenesis, proliferation and differentiation of adipocyte precursors and were identified as responsible for phagocytosis of necrotic adipocytes, forming so-called crown-like structures (CLS) [61]. Their phenotype and function may alter according to a lean/obese and anti-/pro-inflammatory state (Figure 2). In the lean state, most macrophages have an anti-inflammatory (M2 or alternatively activated) phenotype characterized by anti-inflammatory cytokines secretion, such as IL-10 and IL-1 receptor antagonist (IL-1Ra), and CD206 expression [61-64]. Their differentiation and survival depends on IL-4 and IL-13. In obesity, M2 macrophages polarize towards a pro-inflammatory (M1 or classically activated) phenotype having an enhanced pro-inflammatory cytokine production, e.g. TNF-α, IL-6 and IL-12. They express CD11c and their differentiation is promoted by agents such as IFN-γ and lipopolysaccharide (LPS) [61-64].

The numbers of both mast cells and eosinophils in adipose tissue are lower than those of adipose tissue-resident macrophages. Eosinophils were identified as the major producers of IL-4 in adipose tissue, crucial for the survival of M2 macrophages (Figure 2)

[65]. Thereby, in adipose tissue, eosinophil numbers are positively correlated with M2 macrophage numbers [61, 62].

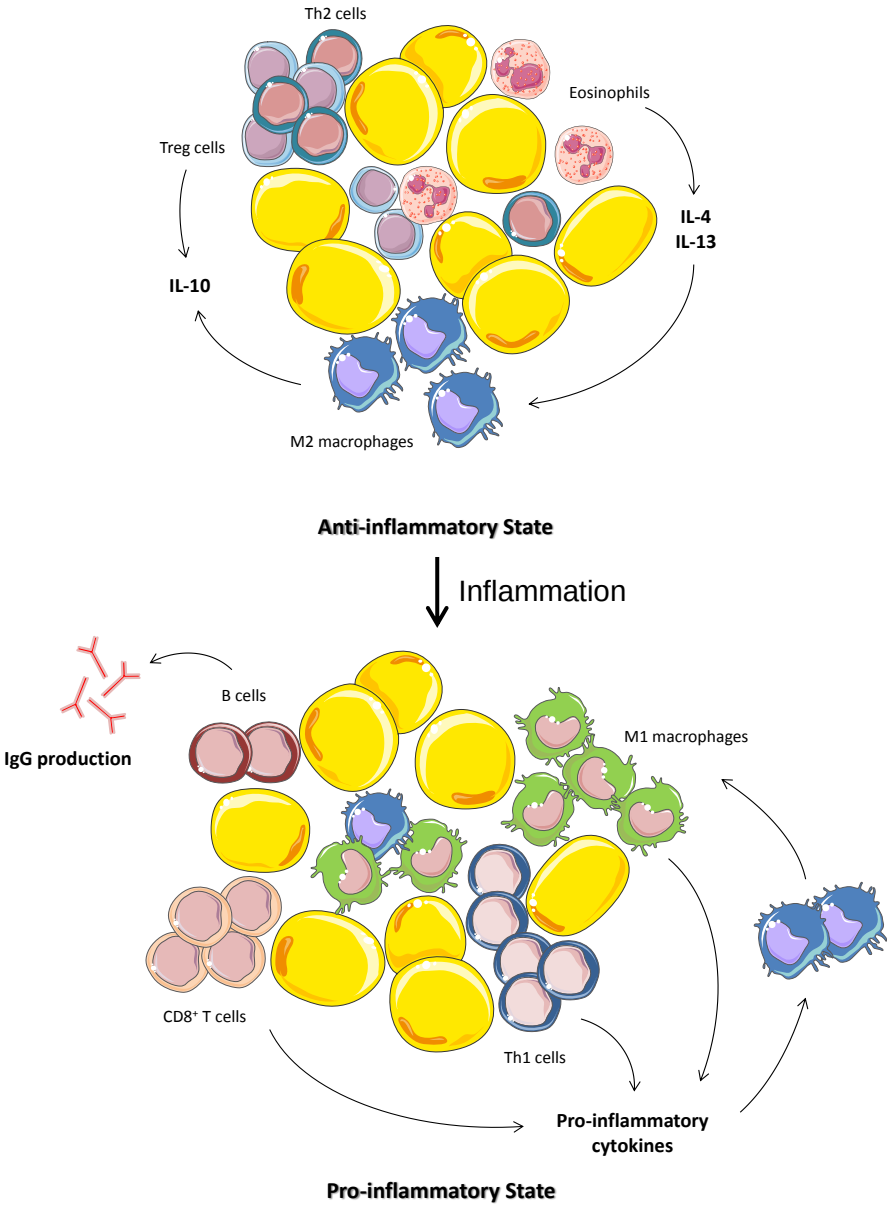

Figure 2. In the anti-inflammatory state, adipose tissue has elevated numbers of Th2 T cells, Treg cells, eosinophils and M2 macrophages. Treg cells secrete IL-10 and eosinophils secrete IL-4 and IL-13, contributing to the anti-inflammatory phenotype. In the onset of inflammation, immune cells are recruited and contribute to further adipose tissue inflammation. M2 macrophages become polarized to pro-inflammatory M1 macrophages, eosinophil and Treg content decreases and there is an increase in Th1 T cells and $CD8^+$ T cells, which secrete pro-inflammatory cytokines. B cell numbers also increase, secreting IgG antibodies.

4.4. Adaptive immunity

B and T lymphocytes infiltrate adipose tissue and play important effector or regulatory roles in organism metabolism. Their number in this tissue correlates with

adiposity, having VAT a greater quantity of T and B lymphocytes per gram in obese subjects [59, 62].

B-2 lymphocytes are present in the VAT of lean mice and secrete antibodies of the IgG isotype (Figure 2) [59].

In what concerns T cells, $CD8^+$, $CD4^+$ and Treg subsets were identified in adipose tissue. The infiltration of $CD8^+$ T cells in adipose tissue seems to contribute to macrophage influx and M1 polarization, which initiates adipose tissue inflammation (Figure 2) [66]. On the other hand, VAT presents more $CD4^+$ T cells that express the Th2 regulating transcription factor GATA3, being these cells somehow important for maintaining immune homeostasis. However, this Th2 phenotype can polarize towards a pro-inflammatory Th1 phenotype, increasing IFN-γ-expressing $CD4^+$ T cells (Figure 2) [59, 61, 62]. Lastly, the presence of Treg cells is important to control inflammation, being the number of this cellular population increased in VAT of young lean subjects and showing a progressive accumulation over time (Figure 2) [55, 59, 62, 67].

4.5. Bridging immunity

There are other subsets of B and T lymphocytes, innate-type B and T cells, that exhibit characteristics qualified to both innate and adaptive immunity. They express B or T cell receptors but are unable to develop immunological memory. In adipose tissue, three subsets of these cells have been described: γδ T cells, invariant natural killer T (iNKT) cells and B-1 B cells.

γδ T cells have regulatory roles in liver and mucosal surfaces by initiating or inhibiting inflammation and by contributing to macrophage homeostasis. Recently, γδ T cells were identified as the main producer of IL-17 in adipose tissue, displaying a possible regulatory role and a cytolytic activity [55, 68].

NKT cells display cell-surface markers typical of NK cells but express the antigen-specific αβ T cell receptor (TCR). Several types of NKT cells have been defined according to their TCR chain and expression of various surface markers, namely iNKT cells, which are CD1d-restricted cells, responding to antigen presentation by non-classical MHC-like antigen presenting molecule CD1d. Adipose tissue-resident iNKT cells represent a considerable fraction of the resident T lymphocyte pool. In the absence of external stimuli, these cells exhibit a Th2-biased cytokine profile, which upon stimulation may produce either pro or anti-inflammatory cytokines [62, 69].

As referred above, B-1 cells are important to confer immunity to bacterial pathogens. They also secrete large amounts of a polyreactive antibody, IgM, which

promotes phagocytosis of apoptotic cells, suggesting an involvement of B-1 cells and macrophages in the clearance of adipocytes [61].

5. Adipose tissue and infectious diseases

The ability of adipose tissue to function as a reservoir for some microorganisms has been previously described. Gray *et al* revealed that the omentum of C57BL6/J mice is a site of chronic murine gammaherpesvirus 68 (MHV68) infection and may contribute to chronic infection [70]. *Mycobacterium tuberculosis* was also shown to enter and persist within adipocytes without apparent replication [71]. Additionally, it has been suggested that mycobacteria sequesters host fatty acids in lipid droplets, which allows its survival in a non-replicating state [72]. Finally, the protozoan causative of Chagas disease, *T. cruzi*, has been subject of several studies. This parasite was demonstrated to invade adipocytes during acute Chagas disease and persist in adipose tissue long after the acute phase has subsided [73]. Adipose tissue obtained from infected CD-1 mice 15 days p.i. revealed a significant increase in macrophage and pro-inflammatory cytokines and a reduction in lipid accumulation, adipocyte size and fat mass, showing a preference of *T. cruzi* for WAT, comparatively to BAT, given the increased levels of free fatty acids or other nutrients essential for the rapid proliferation of the parasite [73, 74].

Aim of the study

The importance of adipose tissue in participating in immune responses and its function as a reservoir for several pathogens has been documented. At present, there are no studies published about the interaction between adipose tissue and *N. caninum*, whether it is a reservoir for this parasite or an important source of immune cells when a host immune response is elicited. In this study we aimed to investigate the role of adipose tissue in host immune response to *N. caninum* infection. Therefore, the focus of this work concerns the presence of macrophages and Treg cells in adipose tissue, since they are known to be important populations in this tissue and be involved in the host immune response against *N. caninum*. The production of IFN-γ and IL-10, known to be responsible for a protective or susceptible host immune response, by several cell populations will also be assessed.

Materials and Methods

1. Mice

Female wild-type (WT) C57BL/6 mice (8-10 weeks old) were obtained from Charles River (Barcelona, Spain) and kept at the animal facilities of Instituto de Ciências Biomédicas Abel Salazar (ICBAS), Porto, Portugal during the experiments. Female IL-12/IL-23 $p40^{-/-}$ ($p40^{-/-}$) C57BL/6 mice were purchased from Jackson Laboratories (Bar Harbor, Maine, USA) and housed and bred also at ICBAS in individual ventilated cages. All procedures involving mice were performed according to the European Convention for the Protection of Vertebrate Animals used for Experimental and Other Scientific Purposes (ETS 123) and 86/609/EEC Directive and Portuguese rules (DL 129/92).

2. *Neospora caninum* tachyzoites

Neospora caninum tachyzoites (NcT) of the Nc1 isolate (Nc-1, ATCC 50843) were cultured and serially passaged in VERO cells maintained at 37 ^{0}C in Minimum Essential Medium (MEM) containing Earle's salts (Sigma-Aldrich, St Louis, MO, USA), supplemented with 10% fetal bovine serum (FBS) (Gibco, Invitrogen Corporation, Carlsbad, California, USA), L-Glutamine (2 mM), penicillin (200 IU/mL) and streptomycin (200 µg/mL) (all from Sigma) in a humidified atmosphere of 5% CO_2 in air. Infected VERO cells were cultured until the host cell monolayer was 90% destroyed and adherent cells were harvested using a cell scraper. Culture supernatants were centrifuged at 1500g for 20 minutes, at 6 ºC. The pellet was passed through a 25G needle and washed three times with Phosphate-Buffered Saline (PBS) (Gibco) by centrifugation at 1500g for 20 minutes. The obtained pellet was suspended in 3 mL of PBS and passed through a PD-10 column filled with Sephadex G-25M (Amersham Biosciences Europe GmbH, Freiburg, Germany). Parasite concentration was determined with a haemocytometer.

3. Challenge infections

N. caninum infections were performed in WT and $p40^{-/-}$ C57BL/6 mice by i.p. inoculation of 1×10^7 tachyzoites in 0,5 mL of PBS. Mock-infected controls were similarly injected with 0,5 mL of PBS.

4. Sample collection

At 6h, 7 days and 2 months after i.p. challenge, mice were euthanized upon isoflurane anesthesia by cervical dislocation. SAT (Figure 3A), gonadal VAT (Figure 3B),

omental VAT (Figure 3C), mesenteric VAT (Figure 3D), IMAT (Figure 3E), liver, spleen, thymus, lungs, heart, pancreas and brain were collected, fixed in 3,7-4,0% formaldehyde (Panreac, Barcelona, Spain), dehydrated and embedded in paraffin wax for usage in histopathology.

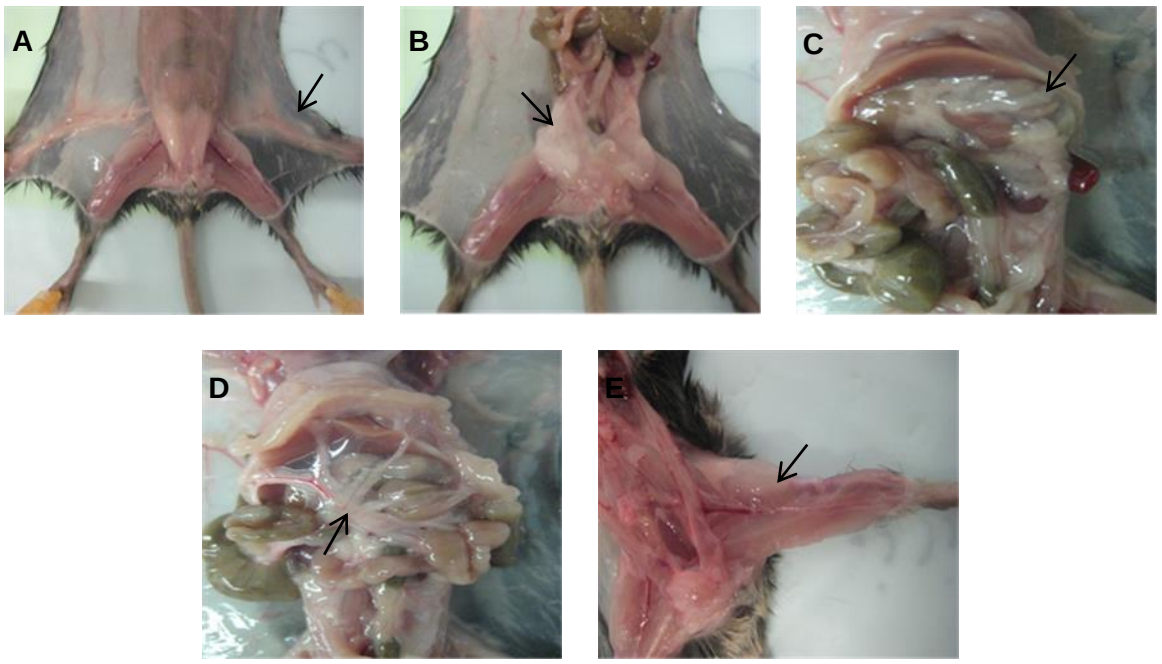

Figure 3. Representative images of (A) SAT, (B) gonadal VAT, (C) omental VAT, (D) mesenteric VAT and (E) IMAT collected from C57BL/6 mice i.p. challenge.

A portion of SAT, gonadal VAT, mesenteric VAT, lung and brain were also collected at 7 days and 2 months after challenge and frozen at -80º C, for DNA extraction.

Additionally, SAT, gonadal VAT, mesenteric VAT and omental VAT were collected and minced into fine pieces and placed in HBSS supplemented with 4% bovine serum albumin (BSA), 10 mM Hepes and collagenase type II (from *Clostridium hystolyticum*) (all from Sigma) at a concentration of 1 mg per mL of the culture medium, for isolation of SVF cells.

5. Histopathology and IHC

Histopathology of tissue samples was assessed in formalin-fixed, paraffin-embedded 4 µm sections, which were cut and mounted on glass slides. All slides were deparaffinized in xylene and rehydrated through a graded series of ethanol solutions, ending in running deionized water.

5.1. *N. caninum* staining

For antigen retrieval, sections were boiled in a pressure cooker with 10 mM Citrate Buffer, pH 6,0, for 2 minutes. The slides were cooled, washed three times and endogenous peroxidase activity blocked with methanol containing 0,3% hydrogen peroxide (H_2O_2) (Merck, Darmstadt, German), for 20 minutes. Sections were incubated in a moist chamber with swine normal serum (Dako), diluted 1:5 in 10% BSA (Sigma), diluted in Tris-buffered saline (TBS, 50 mM Tris, 150 mM NaCl, 0,1% Tween 20, pH=7,6), for 20 minutes at room temperature (RT), to block non-specific binding. Excess serum was drained and replaced with the primary antibody goat anti-*N. caninum* (VMRD, Pullman, WA, USA) diluted 1:2000, for 1 hour and 45 minutes at 37 ^{0}C. Slides were washed and incubated for 30 minutes at RT with the peroxidase-labeled rabbit anti-goat secondary antibody (Millipore, Billerica, MA, USA) diluted 1:1500. Sections were then washed and incubated for 7 minutes at RT with 3,3'-diaminobenzidine (DAB) freshly prepared (Dako), according to manufacturer's instructions. After counterstaining tissue sections with Mayer's Haematoxylin (Merck), they were dehydrated in a graded series of ethanol solutions and xylene and mounted in Entellan mounting medium (Merck). All washes were performed using TBS. Dilution of primary antibody, biotin-labeled secondary antibody and ABC were made in 5% BSA (Sigma) in TBS.

The number of stained cells was assessed by appropriate software (OlyVIA 2.5 – Olympus, USA).

5.2. F4/80 staining

Endogenous peroxidase activity was blocked with methanol containing 0,3% H_2O_2, for 20 minutes, washed three times and incubated in a moist chamber with normal rabbit serum (Dako, Glostrup, Denmark), diluted 1:5 in 10% BSA (Sigma), diluted in PBS/Tween, for 20 minutes at RT. Excess serum was drained and replaced with the primary antibody rat anti-mouse F4/80 (BM8) or the isotype control Rat IgG2a k (both from eBioscience, San Diego, USA) diluted 1:100, for 1 hour and 15 minutes at 37 ^{0}C. Slides were washed and incubated for 30 minutes at RT with the biotin-labeled rabbit anti-rat secondary antibody (Dako) diluted 1:200. After washing, sections were incubated with the Avidin/Biotin Complex (ABC) kit (Vector Laboratories, California, USA) for 30 minutes at RT, washed and incubated for further 7 minutes at RT with DAB. After counterstaining tissue sections with Mayer's Haematoxylin, they were dehydrated in a graded series of ethanol solutions and xylene and mounted in Entellan mounting medium. All washes were performed using PBS with 0,1% of Tween 20 (Sigma). Dilution of primary antibody, biotin-labeled secondary antibody and ABC were made in 5% BSA in PBS/Tween.

To each section, 20 images were acquired, when possible, in a 200x magnification field. Data analysis was accomplished with the image analysis software ImageJ 1.47v (National Institutes of Health, USA) to determinate the frequency of stained area.

5.3. Foxp3 staining

For antigen retrieval, sections were boiled in a pressure cooker with 10 mM Citrate Buffer, pH 6,0, for 2 minutes. The slides were cooled and washed three times and endogenous peroxidase activity was blocked with methanol containing 0,3% H_2O_2, for 20 minutes. Blocking of endogenous biotin activity was performed using the Avidin/Biotin Blocking kit (Vector laboratories), according to manufacturer's instructions. Sections were then incubated in a moist chamber with rabbit normal serum (Dako), diluted 1:5 in 10% BSA diluted in TBS, for 20 minutes at RT. Excess serum was drained and replaced with the primary antibody rat anti-mouse/rat Foxp3 (FJK-16s) or the isotype control Rat IgG2a k (both from eBioscience) diluted 1:100, for 1 hour and 45 minutes at 37 ^{0}C. Slides were washed and incubated for 30 minutes at RT with the biotin-labeled rabbit anti-rat secondary antibody (Dako) diluted 1:200. Sections were then washed and incubated with the ABC kit for further 30 minutes at RT. Finally, slides were washed and incubated for 7 minutes at RT with DAB. After counterstaining tissue sections with Mayer's Haematoxylin, they were dehydrated in a graded series of ethanol solutions and xylene and mounted in Entellan mounting medium. All washes were performed using TBS. Dilution of primary antibody, biotin-labeled secondary antibody and ABC were made in 5% BSA in TBS.

To each section, 20 images were acquired, when possible, in a 20x magnification field. Data analysis was accomplished with the image analysis software ImageJ 1.47v (National Institutes of Health) to determinate the number of stained cells.

6. DNA extraction and real-time PCR analysis

Brain and lung samples were homogenized respectively with 25G needles and glass homogenizers in SE buffer (75 mM NaCl and 25 mM EDTA, pH=8,0). The lysis buffer was complete by adding SDS and proteinase K (Affymetrix USB, Santa Clara, CA, USA) to a final concentration of 1% and 1 mg/mL respectively. Adipose tissue samples were transferred directly to the lysis buffer. Samples were digested overnight at 55 ºC in a water bath, with occasional vigorous mixing. Digested samples were added to a phenol (Sigma)-chloroform (Merck) 1:1 solution, vigorously mixed and centrifuged at 3644g, for 10 minutes, at 6 ºC. The aqueous phases were transferred to a new phenol-chloroform 1:1 solution and the protocol described above was repeated. DNA precipitation was accomplished by slowly mixing the aqueous phases with a solution of cold ethanol (2:1)

and 7,5 M ammonium acetate (1:3) (both from Merck) and letting it rest at -20 ºC. Samples were centrifuged for 15 minutes at 3432g and 6 ºC, pellets were resuspended in cold ethanol and the centrifuged was repeated. DNA pellet was allowed to dry at RT and resuspended in apyrogenic water. Extracted DNA was quantified using the Thermo Scientific NanoDrop 1000 Spectrophotometer and respective software, having the DNA concentration been adjusted to 200 ng/µL for PCR.

To detect *N. caninum* DNA in the collected samples, a Real Time PCR (RT-PCR) was performed using Taqman Probes in a Corbett Rotor Gene 6000 (Corbett life science, Sydney, Australia) device. Product amplification was performed with 1 µL of template DNA in a final volume of 10 µL containing 0,3 µM TaqMan Neo TM probe (FAM CCCGTTCACACACTATAGTCACAAACAAAA-BBQ) (TIBMOLBIOL, Berlin, Germany), 0,2 µM of each primer (forward primer NeoS: 5'-GTTGCTCTGCTGACGTGTCG, reverse primer NeoA: 5'-GCTACCAACTCCCTCGGTT) (TIB-Molbiol, Berlin, Germany) and 1x Rotor-Gene Probe PCR Master Mix (QIAGEN). The PCR program run was as follows: denaturation at 95 ºC for 3 minutes and amplification in 60 cycles (denaturation at 95 ºC for 5 seconds and annealing and extension at 60 ºC, 20 seconds) with fluorescence acquisition.

Quantitative evaluation of fluorescent signals from the PCR products was performed using the Rotor gene 6000 software v1.7 (Corbett life science).

7. Immunofluorescence analysis

Immunofluorescence staining was performed in paraffin-embedded 20 µm tissue sections of gonadal VAT from $p40^{-/-}$ C57BL/6 mice, 6 days after i.p. challenge with *N. caninum*. The slides were deparaffinized in xylene and rehydrated through a graded series of ethanol solutions, ending in running deionized water. They were rinsed in PBS and incubated in a moist chamber for 1h at 37 ºC with 2% BSA (Sigma), 10% FBS (Gibco) and 0,5% saponin (Sigma) in PBS, to eliminate unspecific staining. Excess solution was drained and replaced with the primary antibodies rat anti-mouse CD36 (72-1) (eBioscience) and rabbit anti-*N. caninum* (kindly provided by Dr José Manuel Costa, Centro de Imunologia e Biologia Parasitária Porto, Portugal) diluted at 1:100 or 1:2500, respectively, in a solution of 1% BSA and 0,5% saponin in PBS. The sections were incubated overnight at 4 ºC with primary antibodies. Subsequently, slides were incubated with the secondary antibodies Alexa Fluor 568 goat anti-rat IgG and Alexa Fluor 488 goat anti-rabbit IgG (both from Invitrogen) diluted at 1:1000 in 1% BSA and 0,5% saponin in PBS, for 3h30 at the dark and RT. Tissue sections were mounted in VectaShield mounting medium with 4'-6-diamidino-2-phenylindole (DAPI) to stain the nuclei (H-1200) (Vector)

and cells were analyzed using a laser-scanning confocal microscope (Olympus Fluo View, FV1000, Tokyo, Japan).

8. Isolation of Stromal Vascular Fraction Cells

All adipose tissue samples were digested in a solution of HBSS supplemented with 4% BSA, 10 mM Hepes and collagenase type II (all from Sigma) at a concentration of 1 mg per mL of the culture medium, for 50 minutes in a water bath at 37 ^{0}C, with vortex agitation every 10 minutes. Once digestion was complete, samples were passed through a sterile 100-µm nylon filter and a mechanical digestion was further accomplished using a 25G syringe plunger. The nylon filter was washed with twice of the initial volume of the solution, using a RPMI medium 1640 (Sigma) solution supplemented with 2% FBS (Gibco), 1% Penicillin/Streptomycin (Sigma) and 10 mM Hepes solution (Sigma). The suspension was then transferred to a sterile tube and the number of total leukocytes was determined with Turk's solution (Merck) in a haemocytometer. The suspension was centrifuged at 269g for 10 minutes at 6 ºC and the floating fraction, corresponding to adipose cells, was rejected and the pellet fraction was collected as SVF cells and resuspended in FACS buffer (1x PBS, 2% FBS, 1 mM sodium azide) or a solution of RPMI medium 1640 supplemented with 100 IU/mL penicillin, 50 µg/mL streptomycin, 10 mM Hepes solution, 50 mM 2-mercaptoethanol (all from Sigma) and 10% fetal calf serum (FCS) (Gibco).

9. Cytospin technique and hemacolor staining

Euthanized C57L/6 mice, 6 hours after i.p. infection, were subjected to peritoneal lavage before adipose tissue collection. Isolated SVF cells from adipose tissue samples were submitted to the cytospin technique. 1×10^{5} cells of each sample was pipetted into a plastic chamber after one drop of 30% BSA (Sigma) in PBS and centrifuged at 1000 rpm for 5 minutes in a Cytospin slide centrifuge (Shandon Cytospin 3 Cytocentrifuge). Cells were then fixed in cold methanol for 5 minutes and frozen at -20 ºC until further analysis or subjected to a hemacolor staining. After cellular fixation in methanol, they were kept for 2 minutes in the hemacolor 2 solution and 3 minutes in the hemacolor 3 solution (both from Merck). They were let to dry at RT and mounted in Entellan mounting medium.

10. Flow cytometric analysis

Quantification of different leukocyte populations was performed by flow cytometry analysis in a FACS Canto II flow cytometer (BD Biosciences, San Diego, CA, USA), located in Institute for Molecular and Cell Biology, Porto, Portugal. A number of 1×10^{6}

leukocytes from cell suspensions, obtained as described above, were stained per sample. In order to label dead cells, an eFluor® 450 Fixable Viability Dye (FVD) (eBioscience) was used before surface staining, according to manufacturer's instructions. The following monoclonal antibodies (mAbs) and the respective isotype controls were used: APC-eFluor® 780 anti-mouse F4/80 (BM8), FITC anti-mouse CD4 (RM4-5), APC anti-mouse CD25 (PC61.5), APC-eFluor® 780 anti-mouse NK1.1 (PK136), PE anti-mouse/rat Foxp3 (FJK-16s), PE Rat IgG2a (eBR2a) (all from eBioscience) and Brilliant Violet 510™ anti-mouse CD3 (17A2) (BioLegend). Cells were preincubated with anti-mouse CD16/32 (93) (eBioscience), for 15 minutes before incubation with mAbs for surface staining, for 30 minutes at RT and in the dark. The Foxp3 staining was performed after surface staining using the Foxp3 Staining Buffer Set (eBioscience). Data were analyzed by using FlowJo software, version 9.6.4.

11. Intracellular staining

For cytokine intracellular staining, SVF cells were recovered in supplemented RPMI medium and stimulated for 4,5 hours at 37 ºC with 20 ng/mL phorbol 12-myristate 13-acetate (PMA) (Sigma), 200 ng/mL ionomycin (Calbiochem, San Diego, CA, USA), and 10 µg/mL brefeldin A (Sigma). Cells were preincubated with anti-mouse CD16/32 (93) (eBioscience), for 15 minutes before incubation with mAbs for surface staining, for 30 minutes at RT and in the dark. The following surface mAbs were used: FITC anti-mouse TCR γδ (eBioGL3), APC anti-mouse NK1.1 (PK136), APC-eFluor® 780 anti-mouse CD8a (53-6.7), eFluor® 450 anti-mouse TCRβ (H57-597) (all from eBioscience) and Brilliant Violet 510™ anti-mouse CD4 (RM4-5) (BioLegend, San Diego, CA, USA). Cells were then fixed with 2% formaldehyde (Sigma), washed and permeabilized with 0,5% saponin (Sigma) in FACS. Once again, cellular incubation with anti-mouse CD16/32 (93) (eBioscience) was performed before intracellular staining with the following mAbs, along with the respective isotype controls: PE anti-mouse IL-10 (JES5-16E3), PerCP-Cy5.5 anti-mouse IFN-γ (XMG1.2), PE Rat IgG2a (eBR2a) and PerCP-Cy5.5 Rat IgG1 κ (eBRG1). Data were analyzed by using FlowJo software, version 9.6.4.

12. Statistical analysis

Data is expressed as mean±SD from a *n* number of experiments. Statistical analysis was carried out using unpaired Student's t-test or Mann Whitney test using the GraphPad Prism 6 version 6.02 software (GraphPad, San Diego, CA, USA). *P* values of <0,05 were considered statistically significant.

Results

1. Detection of *N. caninum* tachyzoites in C57BL/6 mice infected by the intraperitoneal route

In order to determine if *N. caninum* infects the adipose tissue early after infection, paraffin-embedded gonadal, mesenteric and omental VAT samples collected from C57BL/6 mice sacrificed 6h after i.p. infection were analyzed by IHC. *N. caninum* was detected in all the depots of adipose tissue analyzed (Figure 4A, B and C).

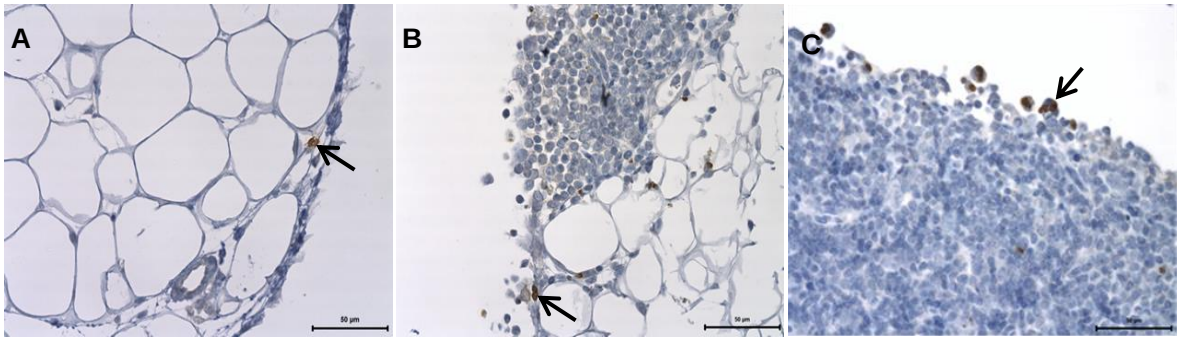

Figure 4. Representative images of *N. caninum* IHC staining in (A) gonadal VAT, (B) mesenteric VAT and (C) omental VAT of C57BL/6 mice infected with 1×10^7 *N. caninum* tachyzoites (NcT) and sacrificed 6h after i.p. challenge. Specific staining (brown) is indicated by arrows and corresponds to NcT.

With the purpose to determine if *N. caninum* could be found in the SVF fraction of adipose tissue, we performed a hemacolor staining of isolated SVF from SAT (Figure 5A), gonadal VAT (Figure 5B), omental VAT (Figure 5C) and mesenteric VAT (Figure 5D).

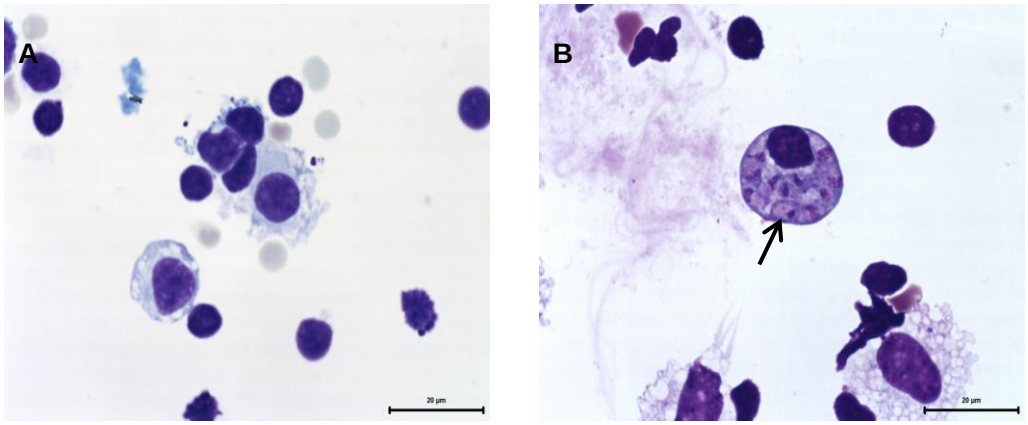

Continues in the following page

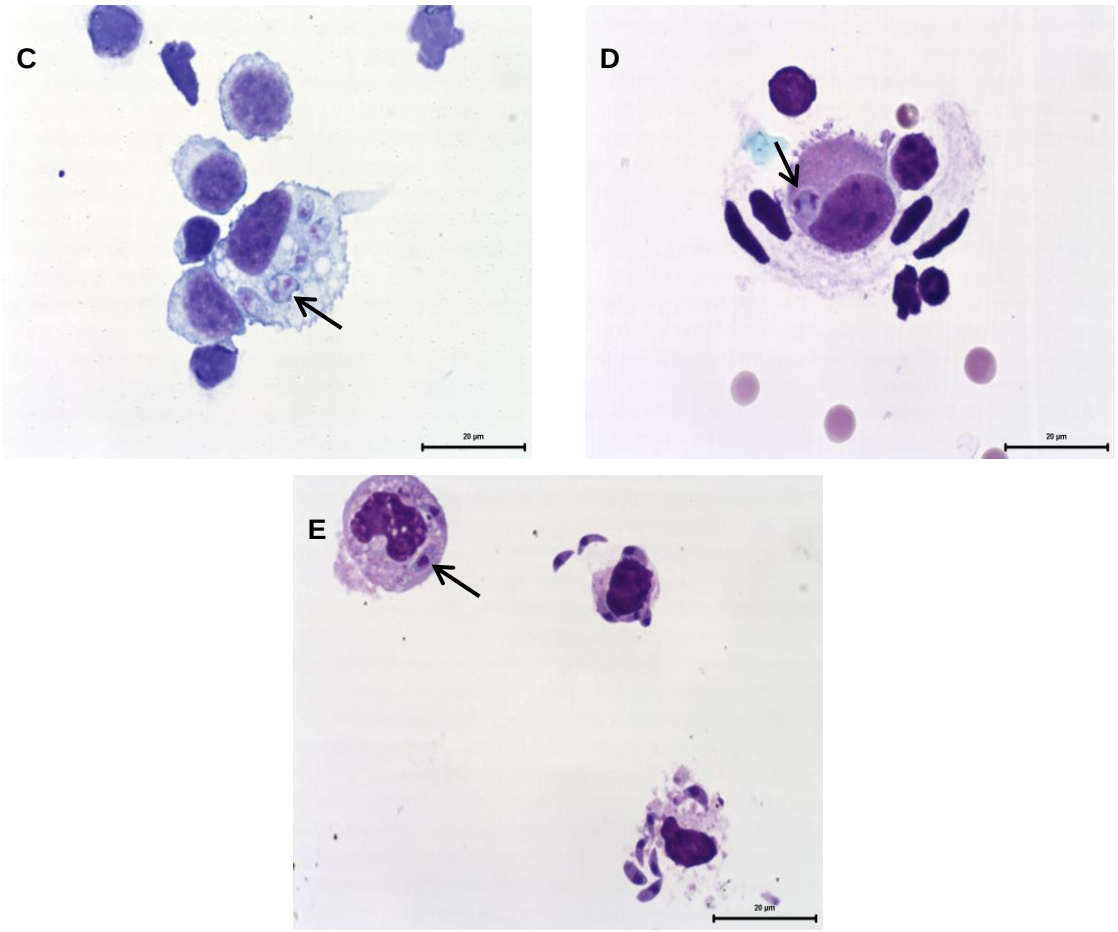

Figure 5. Representative images of hemacolor staining of cells from adipose tissue SVF (A–SAT; B–gonadal VAT; C–omental VAT; D–mesenteric VAT) or cells from (E) peritoneal lavage of infected C57BL/6 mice, sacrificed 6h after i.p. challenge with 1×10^7 NcT. Arrows indicate NcT.

As shown in figure 5, NcT was found within cells, which resemble macrophages, obtained from gonadal, omental, mesenteric VAT and also from peritoneal lavage fluid of infected mice. Contrastingly, the parasite was not detected in SVF from SAT samples.

The presence of *N. caninum* in samples collected from C57BL/6 mice sacrificed 7 days and 2 months after the parasitic i.p. challenge was assessed by RT-PCR and IHC. As shown in figure 6, a significant increase in the number of parasites per µg of host DNA was observed in gonadal and mesenteric VAT, lungs and brain of WT mice 7 days after *N. caninum* infection. No significant difference was observed in SAT samples, were parasitic DNA was detected in only 1 out of 7 infected mice (Figure 6A). Two months after i.p. infection, parasitic DNA was no longer detected by RT-PCR in the depots of adipose tissue analyzed (data not shown).

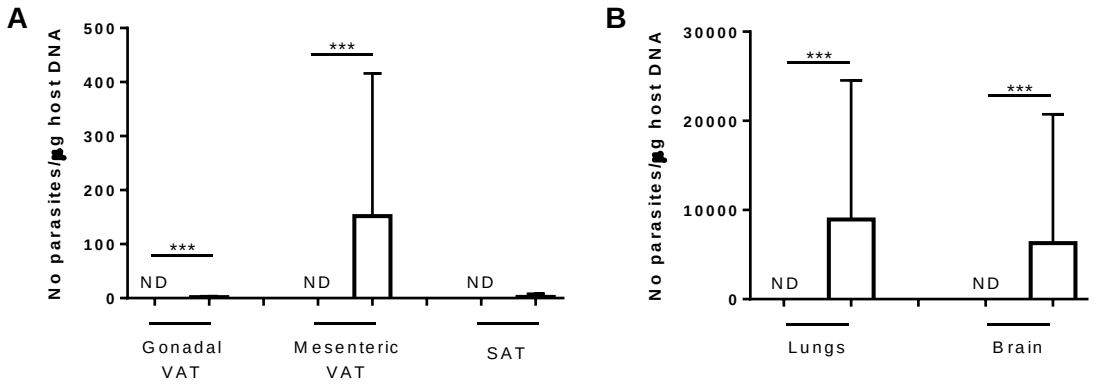

Figure 6. Detection of parasitic DNA by RT-PCR in (A) gonadal VAT, mesenteric VAT, SAT, (B) lung and brain samples of C57BL/6 mice 7 days after i.p. treatment with PBS (■) or inoculation with 1×10^7 NcT (□),. Bars represent mean plus one standard deviation of seven animals per group (***P<0,005).

Since we were able to detect parasitic DNA in tissues of infected mice sacrificed 7 days p.i., an IHC method for *N. caninum* detection was performed, in order to find out the location of the parasite. Results are summarized in Table 1.

Table 1. *N. caninum* IHC analysis in adipose tissue and organs of infected C57BL/6 mice 7 days after i.p. infection.

Tissue sample	Nº of mice positive by IHC/Nº of mice tested
SAT	0/7
Gonadal VAT	0/7
Omental VAT	0/7
Mesenteric VAT	0/7
IMAT	0/7
Liver	0/7
Spleen	1/7
Thymus	0/7
Lung	2/7
Heart	2/7
Pancreas	1/7
Brain	2/7

NcT was not observed in adipose tissue by IHC staining 7 days after i.p. challenge (Table 1). Nevertheless, 7 days p.i., *N. caninum* was detected in several organs, namely spleen, lung, heart, pancreas and brain (Table 1).

Altogether these results show that in C57BL/6 mice, *N. caninum* can disseminate in the host and colonize the adipose tissue, in early stages of infection.

2. Cellular location of *N. caninum* tachyzoites in adipose tissue

Since we have detected *N. caninum* parasites in adipose tissue, we tried to investigate its location in this tissue. With this purpose, we analyzed paraffin-embedded 20 µm tissue sections of gonadal VAT from $p40^{-/-}$ C57BL/6 mice i.p. infected with 1×10^7 tachyzoites by immunofluorescence staining, 6 days after infection.

As shown in figure 7, NcT, stained in green, was easily observed. However, due to the high diameter of each adipocyte, ranging 30-130 µm, weak CD36 staining and insufficient section thickness (20 µm) we were unable to conclude if the parasite is located within or around adipocytes.

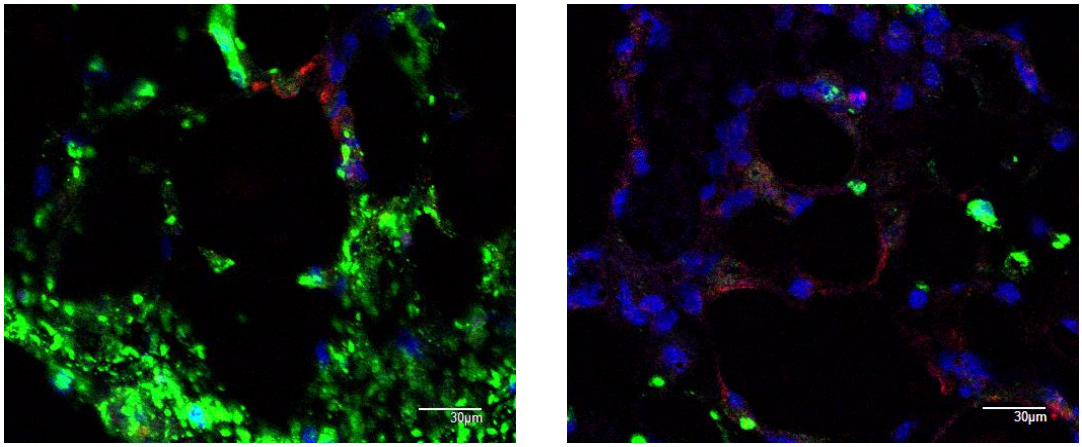

Figure 7. Representative images of immunofluorescence confocal microscopy study of *N. caninum* (green) and CD36 (red) in gonadal VAT of $p40^{-/-}$ C57BL/6 mice infected i.p. with 1×10^7NcT, 6 days after challenge.

3. Characterization of adipose tissue immune response after *N. caninum* infection

As the adipose tissue is populated by immune cells with effector function [61], and *N. caninum* could be found therein upon i.p. infection of C57BL/6 WT mice, we analyzed the immune cell populations present in this tissue and some of the cytokines produced by them, by IHC and flow cytometry.

3.1. Increased number of $F4/80^+$ cells in adipose tissue

Resident and infiltrating adipose tissue macrophages perform a repertoire of functions namely in response to injury and infection, where they phagocyte and kill an array of infectious microorganisms [75]. So, we analyzed this population in the collected adipose tissue using the surface marker F4/80, which is expressed by the majority of mature macrophages.

An analysis of this population on SAT, gonadal VAT, omental VAT, mesenteric VAT and IMAT of control and infected mice, collected 7 days and 2 months p.i., was performed by IHC. Figure 8 is a representative example of F4/80 IHC staining in tissue samples from mice sacrificed 7 days after challenge.

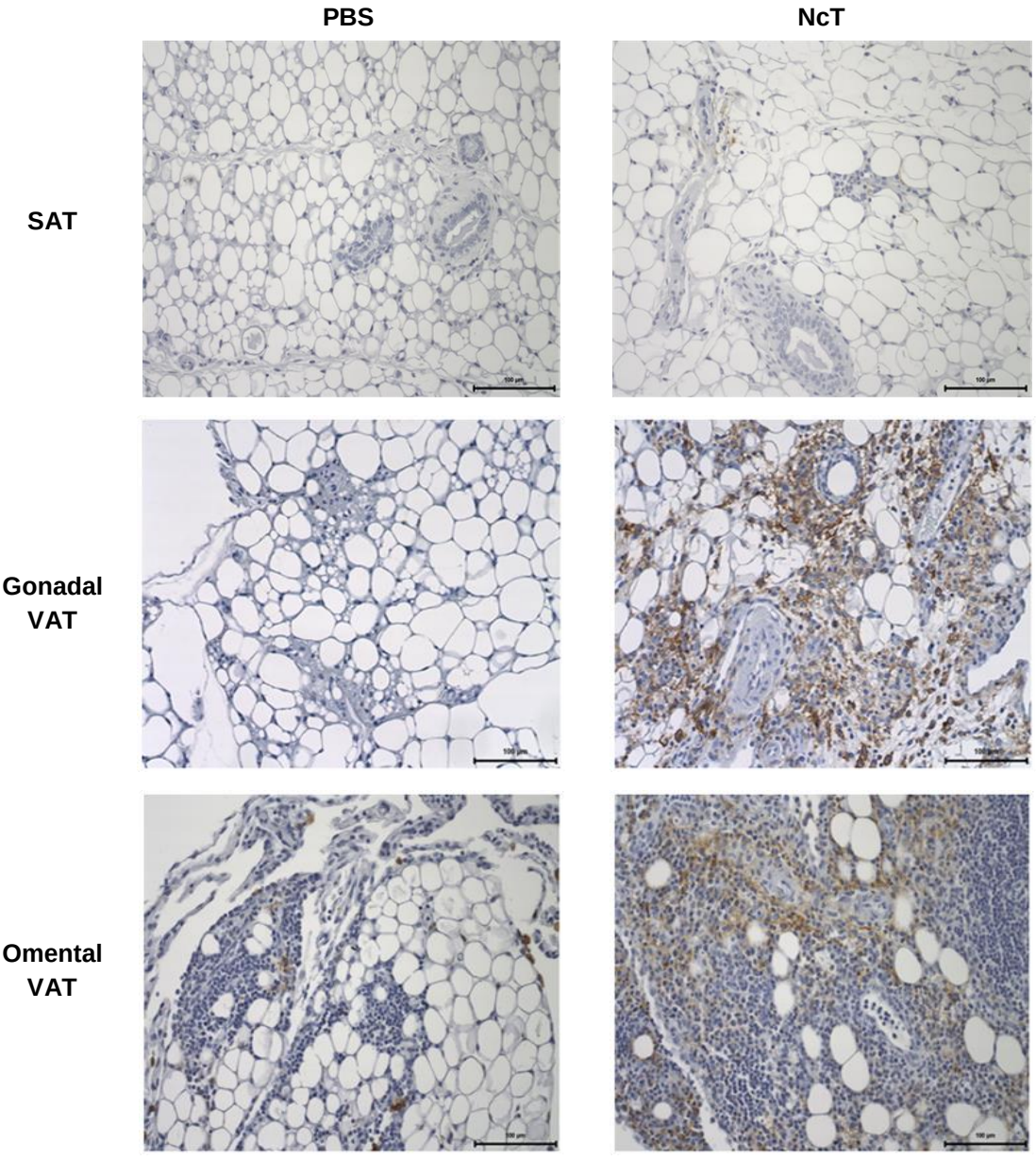

Continues in the following page

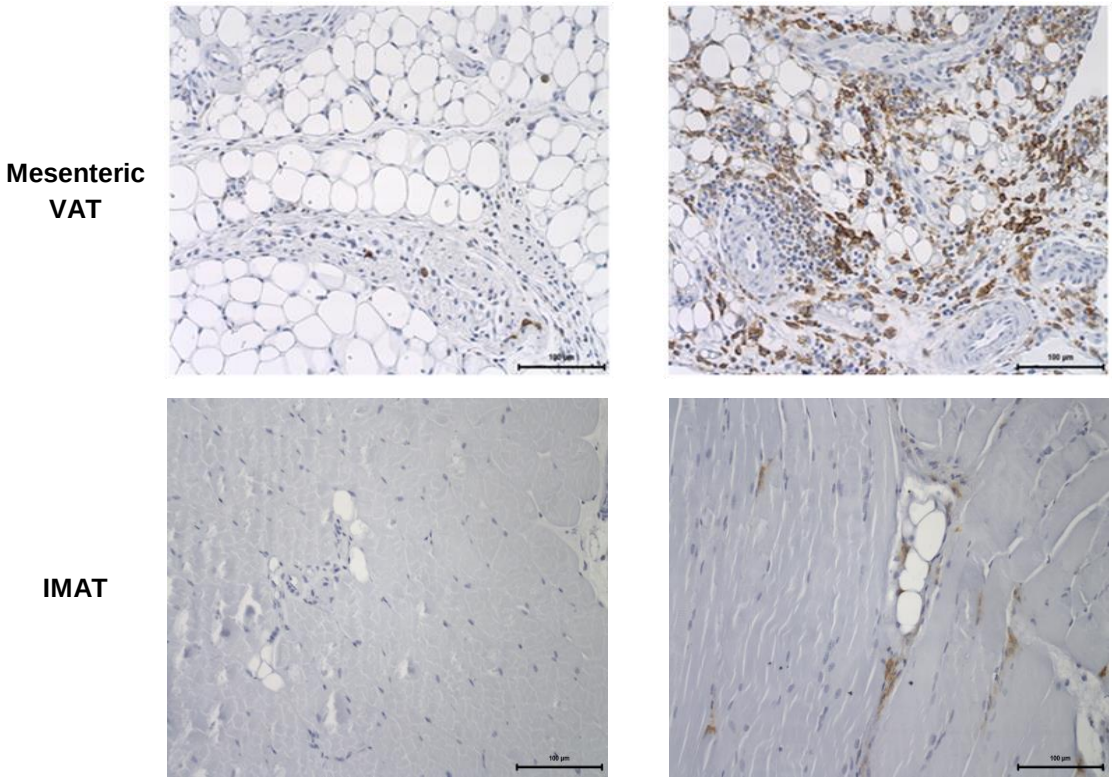

Figure 8. Representative images of immunohistochemistry analysis of F4/80 staining. SAT, gonadal VAT, omental VAT, mesenteric VAT and IMAT from C57BL/6 mice sacrificed 7 days after i.p administration of PBS (PBS) or challenged with 1×10^7 NcT (NcT) were specific stained with a monoclonal antibody anti-F4/80. Brown color corresponds to $F4/80^+$ cells.

As IHC analysis shows, a significant increase in the frequency of $F4/80^+$ stained area was observed in gonadal, omental and mesenteric VAT and IMAT, while no significant differences were observed in SAT of infected mice sacrificed 7 days post i.p. challenge (Figure 9A), comparatively to non-infected control mice. No differences were observed 2 months p.i. in all depots of adipose tissue analyzed (Figure 9B).

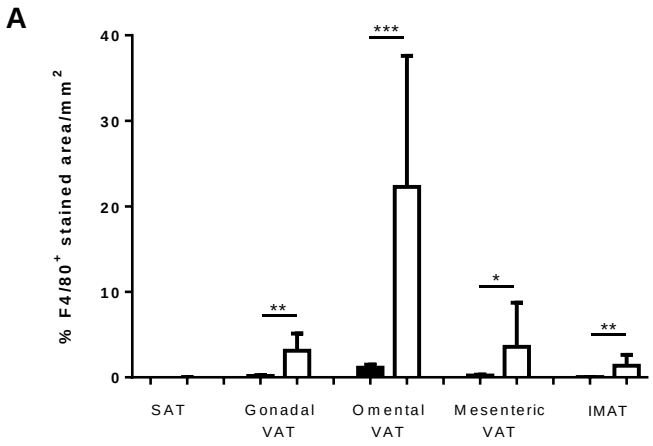

Continues in the following page

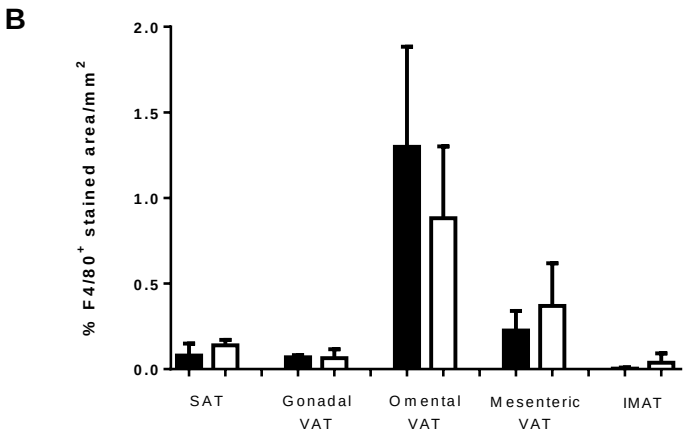

Figure 9. Frequency of F4/80$^+$ stained area per mm^2 of analyzed SAT, gonadal VAT, omental VAT, mesenteric VAT and IMAT, evaluated by IHC, at (A) 7 days and (B) 2 months p.i. in PBS (■) and *N. caninum* i.p.-infected mice with 1×10^7 tachyzoites (□). Bars represent mean plus one standard deviation of seven animals per group in A and three animals per group in B. Statistical significant differences between groups is indicated (**P*<0,05; ***P*<0,01; ****P*<0,005).

In order to assess the number of macrophages in adipose tissue, we isolated SVF from SAT, gonadal, omental and mesenteric VAT, 7 days after i.p. challenge, and analyzed the number of F4/80$^+$ cells by flow cytometry (Figure 10).

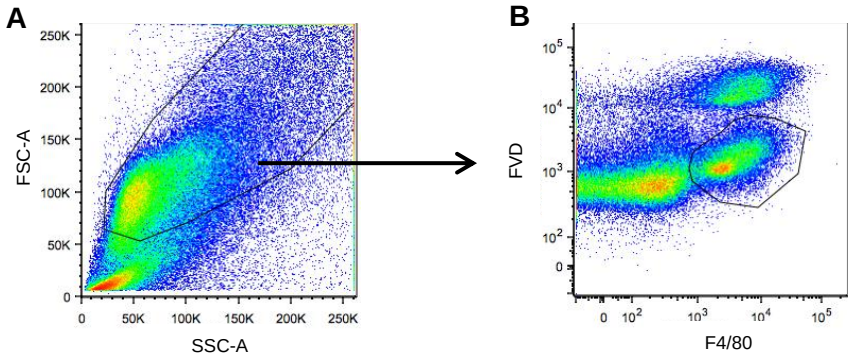

Figure 10. Representative dot plot of isolated SVF fraction from omental VAT of infected C57BL/6 mice. Total adipose leucocytes were gated as shown in A and macrophages were selected as (B) F4/80$^+$FVD$^-$ cells.

A significantly increase in the number of F4/80$^+$ cells from gonadal, omental and mesenteric VAT of NcT challenged mice was observed when compared to non-infected controls (Figure 11). No differences were observed in the number of cells of this population in SAT samples of infected mice, as compared to non-infected controls (Figure 11).

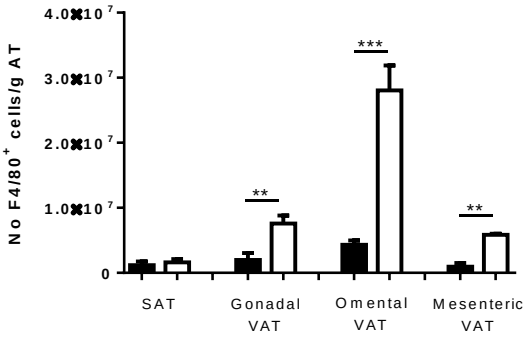

Figure 11. Number of F4/80$^+$ cells from isolated SVF cells per gram of adipose tissue (AT) from control (■) or mice infected with 1×10^7 NcT (□), 7 days after challenge. Bars represent mean plus one standard deviation of three animals per group. Statistical significant differences between groups is indicated (**P<0,01; ***P<0,005).

These results indicate that macrophages respond to *N. caninum* infection and migrate to or proliferate in the adipose tissue contributing to eradicate the infection therein.

3.2. Increased number of Treg cells in adipose tissue

It was previously reported that *N. caninum* infection induces an expansion of spleen CD4$^+$CD25$^+$Foxp3$^+$ T cells in mice [41]. Thus, we assessed Treg cell numbers on the several adipose tissues, collected 7 days and 2 months after the parasitic challenge, by using an IHC method with an anti-Foxp3 monoclonal antibody. Figure 12 is a representative example of Foxp3 staining in tissue samples from mice sacrificed 7 days after challenge.

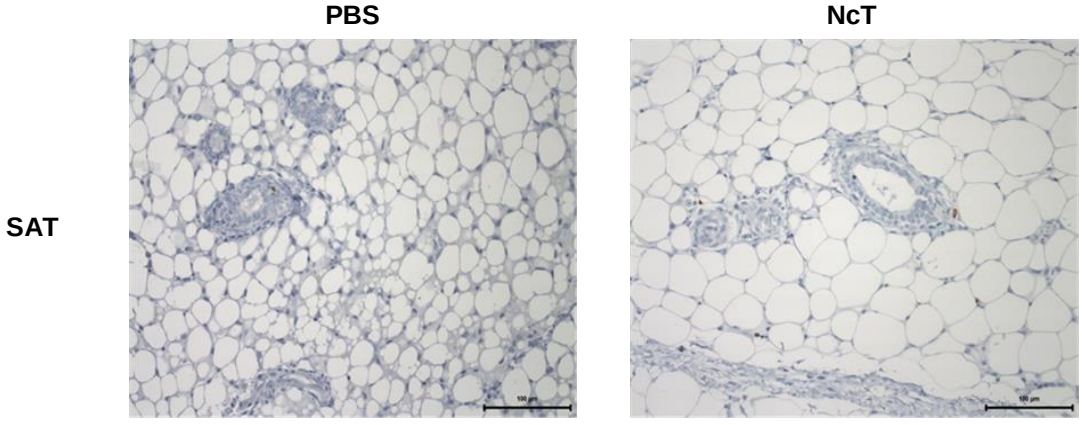

Continues in the following page

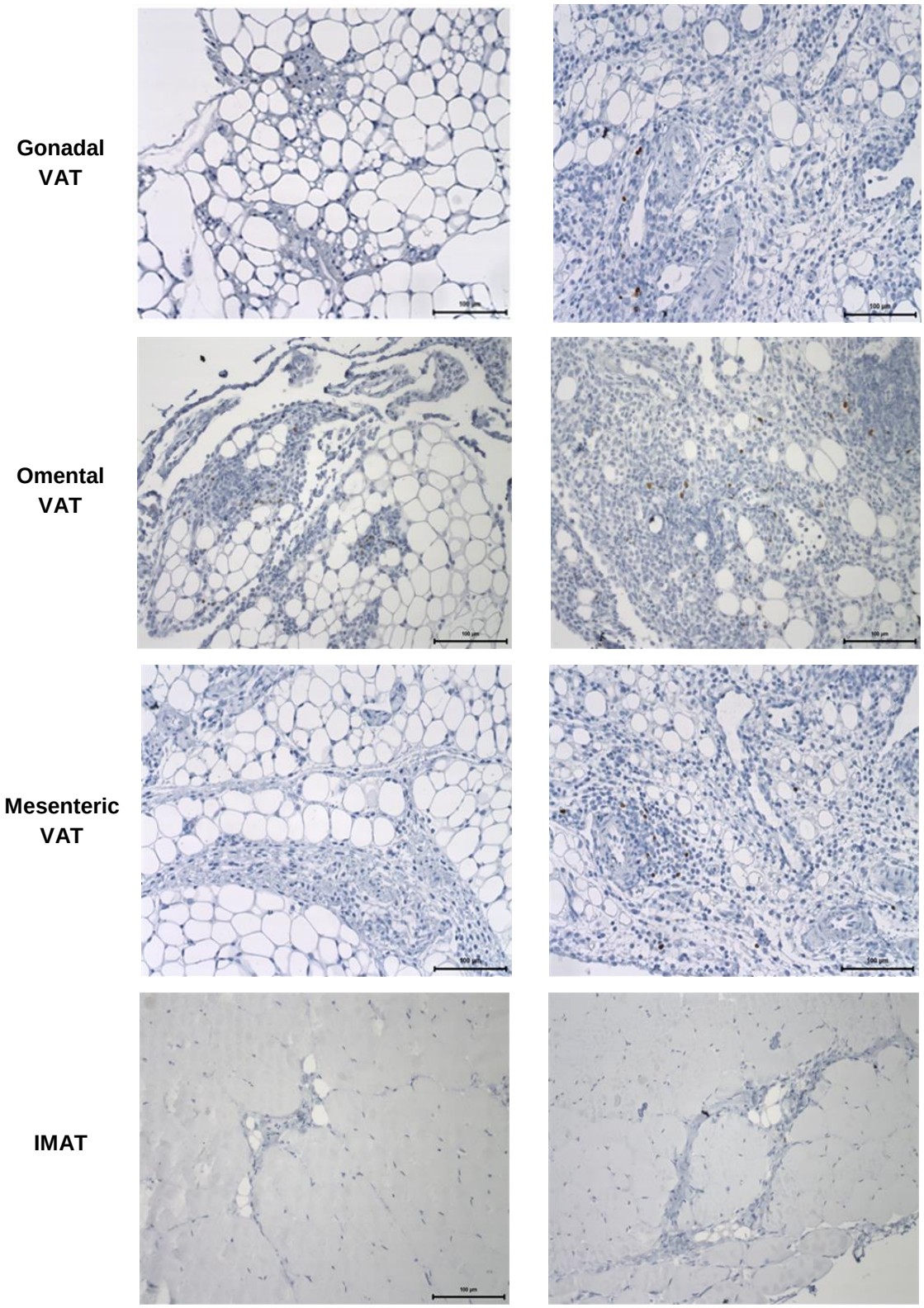

Figure 12. Representative images of Foxp3 staining by immunohistochemistry. SAT, gonadal VAT, omental VAT, mesenteric VAT and IMAT from control (PBS) and infected (NcT) C57BL/6 mice sacrificed 7 days after i.p. challenge were analyzed by immunohistochemistry staining with a monoclonal antibody Foxp3. Specific staining (brownish) corresponds to $Foxp3^+$ cells.

We observed a significant increase in $Foxp3^+$ cells number only in gonadal, omental and mesenteric VAT from infected C57BL/6 mice, sacrificed 7 days upon

challenge (Figure 13A). Foxp3$^+$ cells number was found not to differ between controls and infected mice in SAT and IMAT, 7 days upon infection (Figure 13A), and in the analyzed adipose tissue samples, 2 months upon infection (Figure 13B).

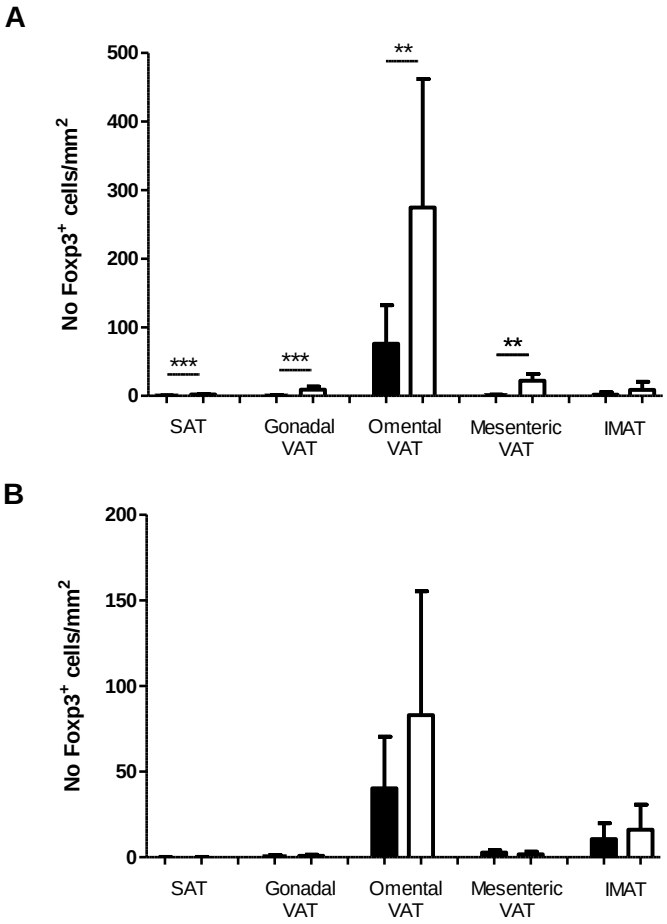

Figure 13. Number of Foxp3$^+$ cells per mm^2 of analyzed SAT, gonadal VAT, omental VAT, mesenteric VAT and IMAT, evaluated by IHC, at (A) 7 days and (B) 2 months p.i., in PBS (■) and *N. caninum* i.p.-infected mice with 1×10^7 tachyzoites (□). Bars represent mean plus one standard deviation of seven animals per group in A and three animals per group in B. Statistical significant differences between groups is indicated (**P<0,01; ***P<0,005).

To further assess the Treg cell population, we analyzed the number and frequency of CD4$^+$CD25$^+$Foxp3$^+$ T cells by flow cytometry, 7 days after i.p. challenge. The dot plots in figure 14 show the regions used to define the CD4$^+$CD25$^+$ and Treg T cell populations.

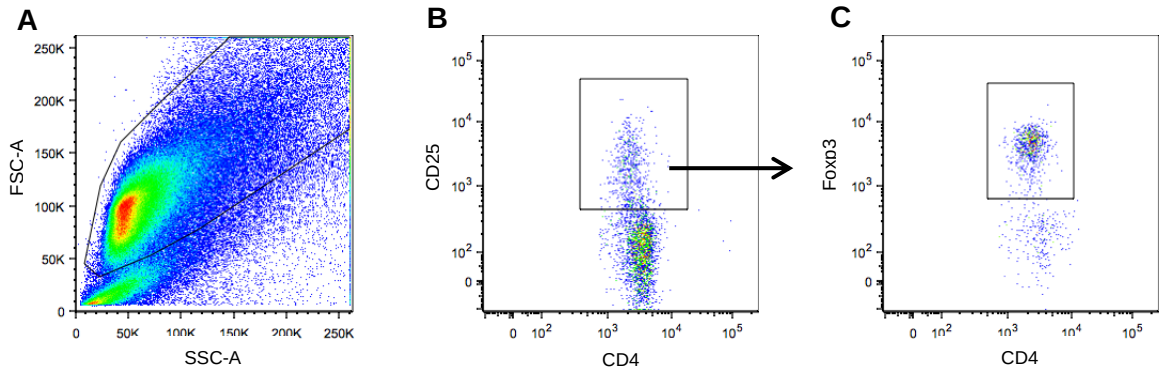

Figure 14. Representative dot plots of isolated SVF fraction from omental VAT of control C57BL/6 mice. (A) Total leukocyte cells, (B) $CD4^+CD25^+$ T cell population gated in $CD3^+CD4^+$ cells, (C) CD4+ Foxp3+ cells gated in $CD4^+CD25^+$ T cells.

As shown in figure 15A, a significant increase in the number of $CD4^+CD25^+Foxp3^+$ T cell in gonadal, omental and mesenteric VAT was observed 7 days after i.p. challenge with *N. caninum*, as compared to controls. Such difference was not detected in SAT from the same mice. Regarding frequencies of $CD4^+CD25^+Foxp3^+$ T cell, it was detected a decrease in SAT, gonadal and omental VAT where there was no difference in mesenteric VAT from parasite-challenged mice (Figure 15B).

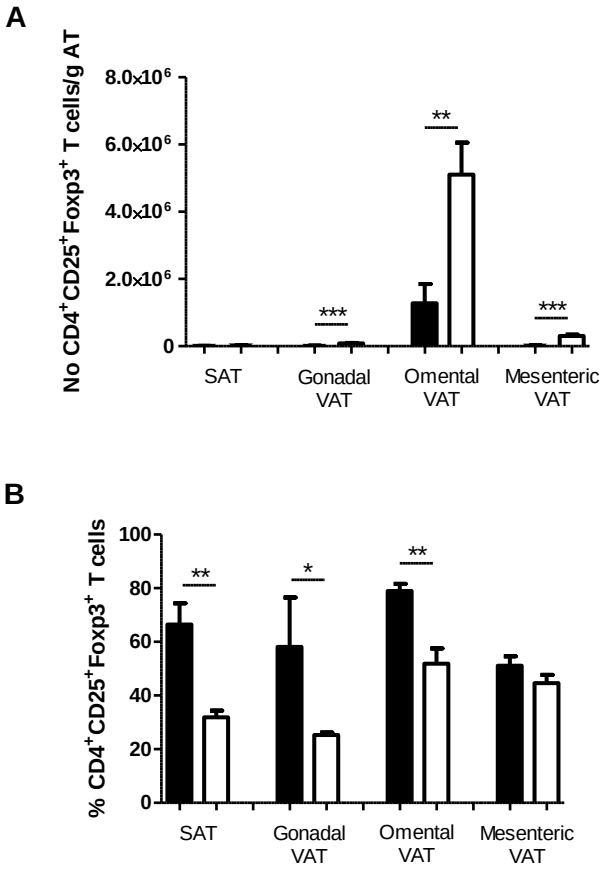

Figure 15. Number per gram of AT (A) and frequency (B) of $CD4^+CD25^+Foxp3^+$ T cells in $CD4^+CD25^+$ T cells of adipose tissue SVF, detected in PBS i.p.-treated (■) or *N. caninum* i.p.-infected mice with 1×10^7 tachyzoites (□), 7 days after

challenge. Bars represent mean plus one standard deviation of three animals on each group. Statistical significant differences between groups is indicated (*P<0,05; **P<0,01; ***P<0,005).

The number and frequency of effector T cells, defined as $CD4^+CD25^+Foxp3^-$ T cells, was also assessed. It was observed a significant increase in $CD4^+CD25^+Foxp3^-$ T cell numbers (Figure 16A) in gonadal, omental and mesenteric VAT samples and in the frequency of these cells (Figure 16B) in SAT, gonadal, omental and mesenteric VAT of infected mice, as compared to controls. No differences were found either in the number of effector T cells in SAT or in the frequency of those in mesenteric VAT of infected mice, 7 days after infection.

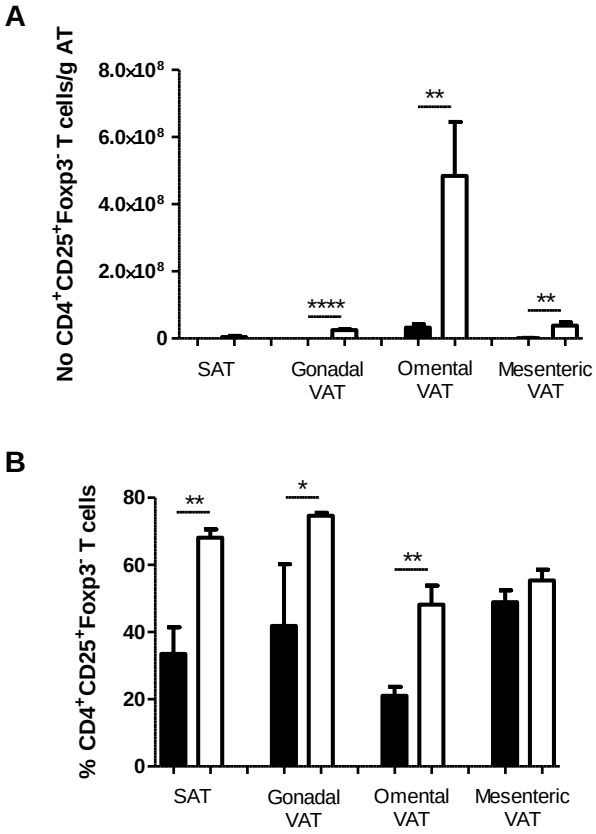

Figure 16. Number per gram of AT (A) and frequency (B) of $CD4^+CD25^+Foxp3^-$ T cells in $CD4^+CD25^+$ T cells of adipose tissue SVF, detected in PBS i.p.- treated (■) or *N. caninum* i.p.-infected mice with 1×10^7 tachyzoites (□), 7 days after challenge. Bars represent mean plus one standard deviation of three animals on each group. Statistical significant differences between groups is indicated (*P<0,05; **P<0,01; ****P<0,001).

Taken together, these data show an expansion of both Treg cell and effector T cell population in the adipose tissue of *N. caninum* infected mice.

4. Cytokine production by adipose tissue immune cell populations

4.1. Analysis of IFN-γ production by NK1.1^{+} cells in adipose tissue

Knowing that NK cells play an integral role in host resistance against parasitic protozoa [25], we studied this cellular population and the production of IFN-γ, a pro-inflammatory cytokine, in adipose tissue of C57BL/5 mice i.p. challenged. A representative example of the gates used to define NK1.1^{+} and NK1.1^{+}IFN-γ^{+} cell populations is shown in figure 17.

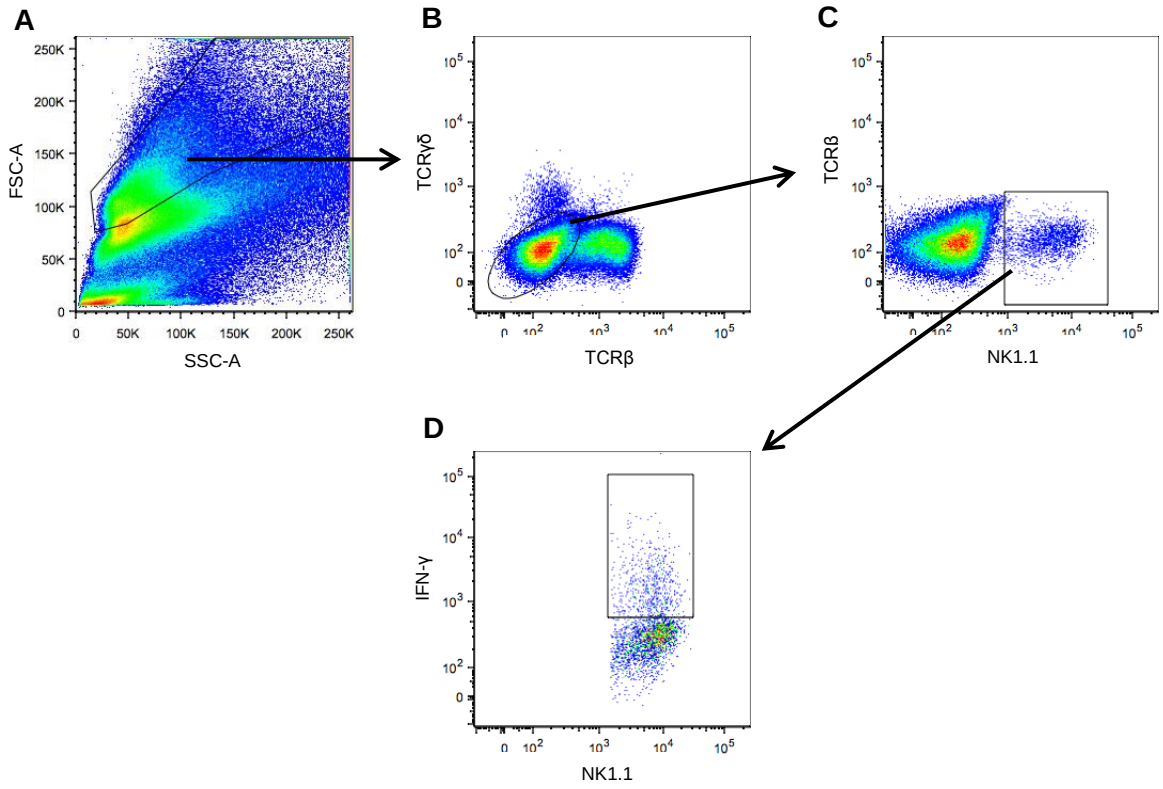

Figure 17. Representative dot plots of isolated SVF fraction from omental VAT of infected C57BL/6 mice. (A) Total leukocyte cells, (B) TCRβ^{-}TCRγδ^{-} cell population gated in A, (C) TCRβ^{-}NK1.1^{+} T cell population gated in TCRβ^{-}TCRγδ^{-} cells, (D) NK1.1^{+}IFN-γ^{+} cells gated in TCRβ^{-}NK1.1^{+} T cells.

The number of NK cells was found increased in SAT, gonadal and mesenteric VAT of infected mice, 7 days after infection. No differences were found in this cell population between omental VAT of control and infected mice (Figure 18).

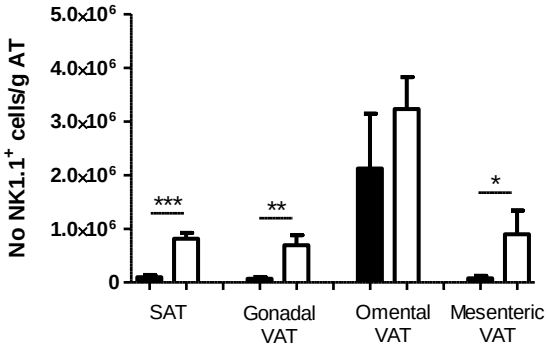

Figure 18. Number of NK1.1$^+$ cells in isolated adipose tissue SVF, detected in PBS i.p.-treated (■) or *N. caninum* i.p.-infected mice with 1×10^7 tachyzoites (□), 7 days after challenge. Bars represent mean plus one standard deviation of three animals on each group. Statistical significant differences between groups is indicated (**P*<0,05; ***P*<0,01; ****P*<0,005).

An increased frequency and number of adipose tissue NK1.1$^+$ cells producing host-protective cytokine IFN-γ in infected mice was observed only in the SAT (Figure 19 and Table 2). The frequency of these cells in the gonadal, omental and mesenteric VAT was not found different between control and infected mice (Figure 19). NK1.1$^+$IFN-γ$^+$ cell numbers per g of adipose tissue were also higher in gonadal and mesenteric VAT from infected mice than in respective controls. This difference was not observed in omental VAT (Table 2).

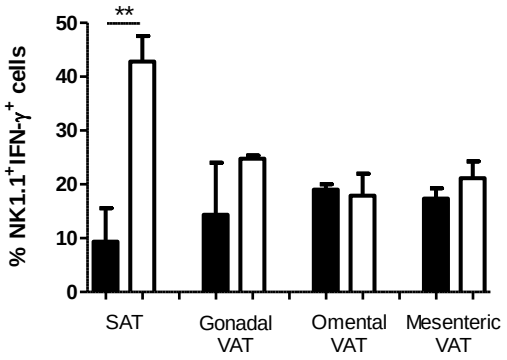

Figure 19. Frequency of NK1.1$^+$IFN-γ$^+$ cells in isolated adipose tissue SVF, detected in PBS i.p.-treated (■) or *N. caninum* i.p.-infected mice with 1×10^7 tachyzoites (□), 7 days after challenge. Bars represent mean plus one standard deviation of three animals on each group. Statistical significant differences between groups is indicated (***P*<0,01).

Table 2. Number of NK1.1$^+$IFN-γ$^+$ cells in isolated adipose tissue SVF, detected in PBS i.p.-treated or *N. caninum* i.p.-infected mice with 1×10^7 tachyzoites, 7 days after challenge. Results are present as mean plus one standard deviation of three animals on each group. Statistical significant differences between groups is indicated (**P*<0,05; ***P*<0,01; ****P*<0,005).

Nº of NK1.1$^+$ cells/g AT x 10^3		**SAT**	**Gonadal VAT**	**Omental VAT**	**Mesenteric VAT**
IFN-γ$^+$	**PBS**	7,41±4,11	11,70±12,36	403,67±188,03	13,93±7,98
	NcT	349,00±66,01***	172,33±48,35**	594,00±242,19	190,00±92,42*

4.2. Analysis of IFN-γ production by TCRγδ$^+$ cells in adipose tissue

γδ T cells play an important role in early immune responses with abundant IFN-γ production [76]. As these cells are known to be a part of the SVF of adipose tissue, we analyzed this population and their IFN-γ production therein. In figure 20 an example of the gates used to define both populations is shown.

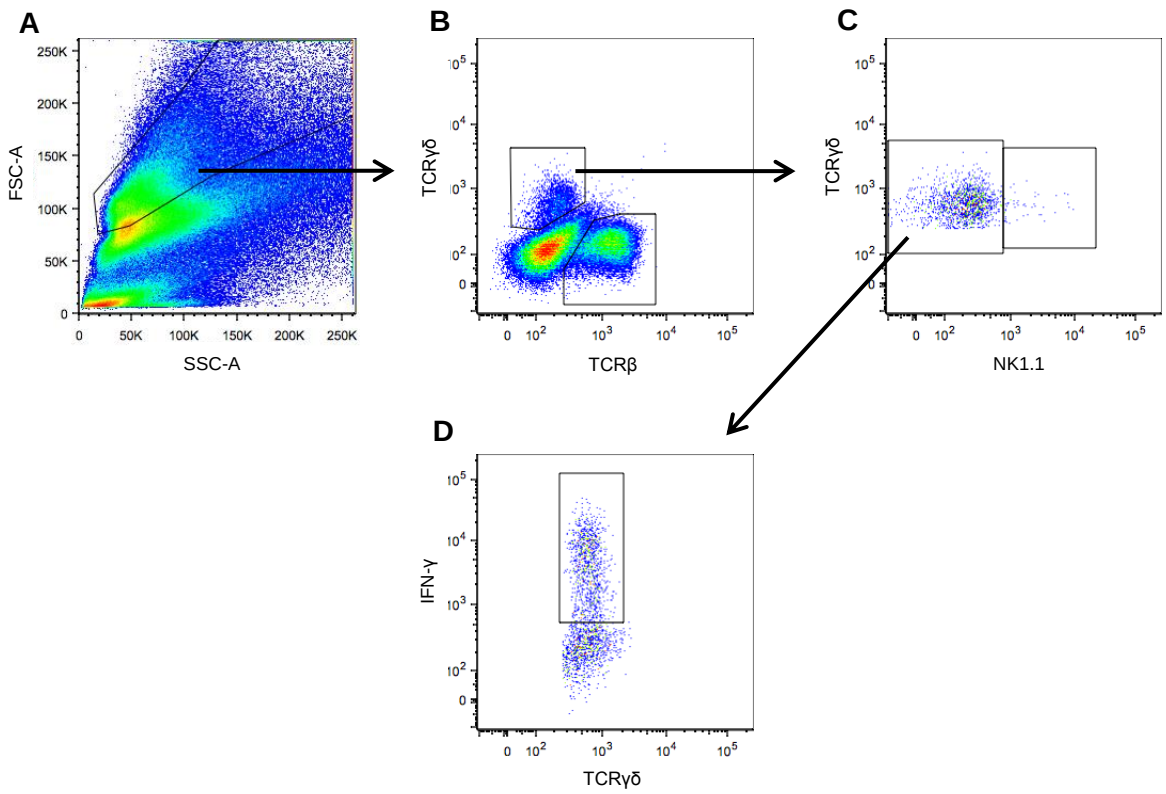

Figure 20. Representative dot plots of isolated SVF fraction from omental VAT of infected C57BL/6 mice. (A) Total leukocyte cells, (B) TCRβ$^-$TCRγδ$^+$ cell population gated in A, (C) TCRγδ$^+$NK1.1$^-$ T cell population gated in TCRβ$^-$TCRγδ$^+$ cells, (D) TCRγδ$^+$IFN-γ$^+$ cells gated in TCRβ$^+$NK1.1$^+$ T cells.

In the four types of adipose tissue analyzed an increase in the number of TCRγδ$^+$ T cells was observed 7 days after infection (Figure 21).

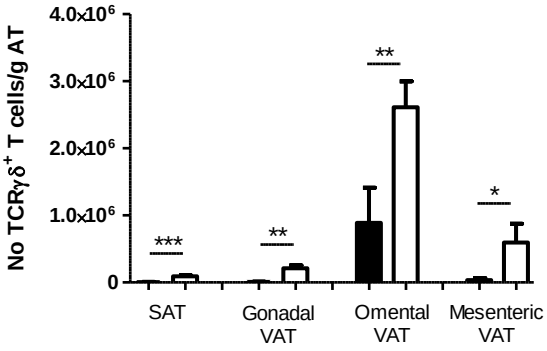

Figure 21. Number of TCRγδ$^+$ T cells in isolated adipose tissue SVF, detected in PBS i.p.-treated (■) or *N. caninum* i.p.-infected mice with 1×10^7 tachyzoites (□), 7 days after challenge. Bars represent mean plus one standard deviation of three animals on each group. Statistical significant differences between groups is indicated (**P*<0,05; ***P*<0,01; ****P*<0,005).

The frequency and number of TCRγδ$^+$ T cells producing IFN-γ was also found increased in the analyzed adipose tissue of infected mice, comparatively to controls (Figure 22 and Table 3).

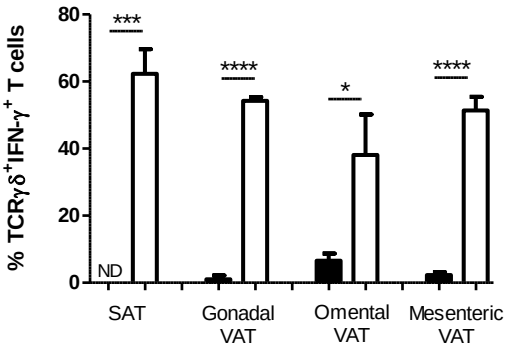

Figure 22. Frequency of TCRγδ$^+$IFN-γ$^+$ T cells in isolated adipose tissue SVF, detected in PBS i.p.-treated (■) or *N. caninum* i.p.-infected mice with 1×10^7 tachyzoites (□), 7 days after challenge. Bars represent mean plus one standard deviation of three animals on each group. Statistical significant differences between groups is indicated (**P*<0,05; ****P*<0,005; *****P*<0,0001).

Table 3. Number of TCRγδ$^+$IFN-γ$^+$ T cells in isolated adipose tissue SVF, detected in PBS i.p.-treated or *N. caninum* i.p.-infected mice with 1×10^7 tachyzoites, 7 days after challenge. Results are present as mean plus one standard deviation of three animals on each group. Statistical significant differences between groups is indicated (**P*<0,05; ***P*<0,01; *****P*<0,0001).

No of TCRγδ$^+$ cells/g AT x 10^3		**SAT**	**Gonadal VAT**	**Omental VAT**	**Mesenteric VAT**
IFN-γ$^+$	**PBS**	0,00±0,00	0,11±0,12	52,83±18,49	0,90±0,94
	NcT	56,13±4,80****	114,40±26,24**	1024,00±435,49*	312,33±169,95*

4.3. Analysis of IFN-γ and IL-10 production by TCRβ$^+$NK1.1$^+$ T cells in adipose tissue

NKT cells are thought to polarize the local and systemic adaptive immune responses to either a pro-inflammatory (IFN-γ) or an anti-inflammatory profile (IL-4 and IL-10) [77]. In this study we assessed the number of cells of this population and their production of IFN-γ and IL-10. A representative example of the gates used to define TCRβ$^+$NK1.1$^+$ T cell population and assessed cytokines is shown in figure 23.

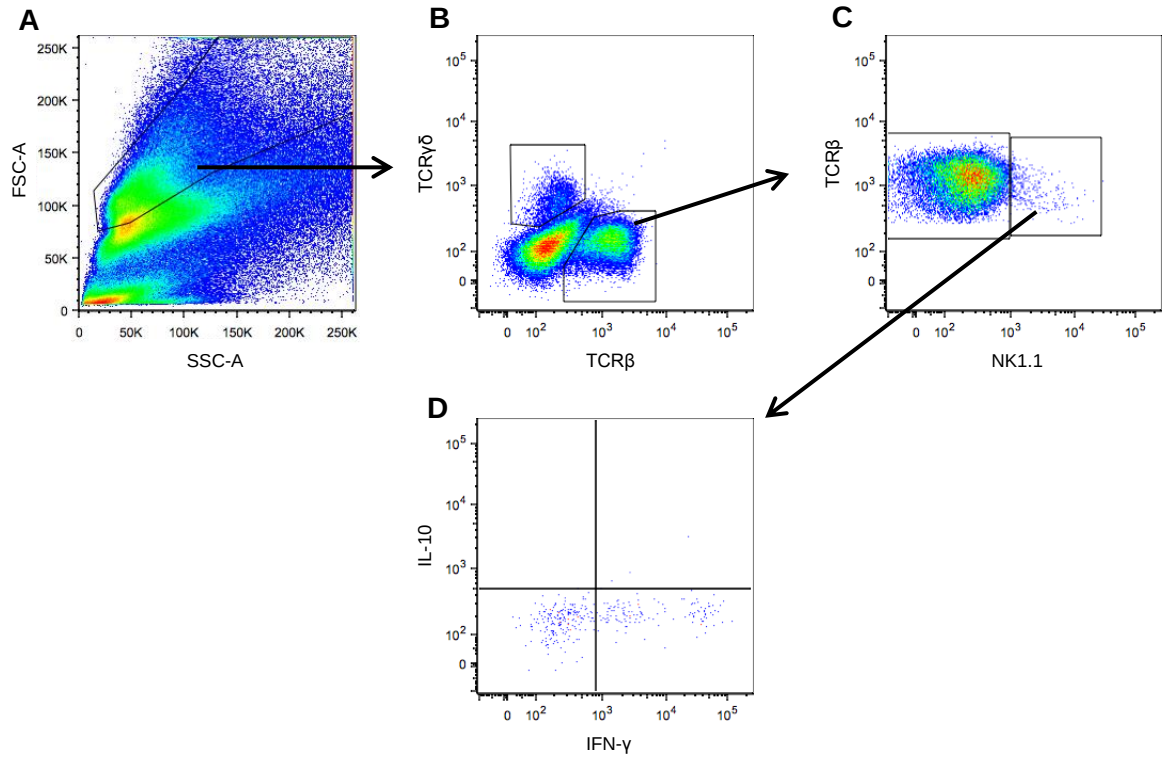

Figure 23. Representative dot plots of isolated SVF fraction from omental VAT of infected C57BL/6 mice. (A) Total leukocyte cells, (B) TCRβ$^+$TCRγδ$^-$ cell population gated in A, (C) TCRβ$^+$NK1.1$^+$ T cell population gated in TCRβ$^+$TCRγδ$^-$ cells, (D) TCRβ$^+$ NK1.1$^+$ T cells expressing IFN-γ and IL-10.

The number of NKT cells in infected mice was found increased in SAT, gonadal and mesenteric VAT and significantly decreased in omental VAT, as compared to controls (Figure 24).

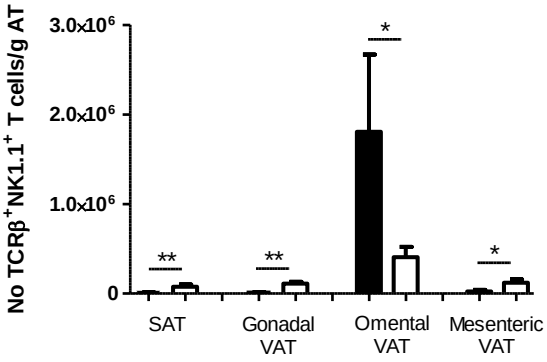

Figure 24. Number of TCRβ$^+$NK1.1$^+$ T cells in isolated adipose tissue SVF, detected in PBS i.p.-treated (■) or *N. caninum* i.p.-infected mice with 1×10^7 tachyzoites (□), 7 days after challenge. Bars represent mean plus one standard deviation of three animals on each group. Statistical significant differences between groups is indicated (*P<0,05; **P<0,01).

No IL-10 production by TCRβ$^+$NK1.1$^+$ cells was detected (data not shown). Conversely, TCRβ$^+$NK1.1$^+$ T cells were found to produce IFN-γ, even though the frequency of adipose tissue TCRβ$^+$NK1.1$^+$IFN-γ$^+$IL-10$^-$ T cells did not differ between control and infected mice (Figure 25).

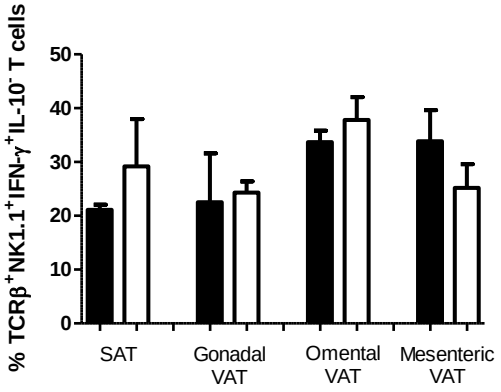

Figure 25. Frequency of TCRβ$^+$NK1.1$^+$IFN-γ$^+$IL-10$^-$ T cells in isolated adipose tissue SVF, detected in PBS i.p.-treated (■) or *N. caninum* i.p.-infected mice with 1×10^7 tachyzoites (□), 7 days after challenge. Bars represent mean plus one standard deviation of three animals on each group. Statistical significant differences between groups is indicated.

The number of TCRβ$^+$NK1.1$^+$IFN-γ$^+$IL-10$^-$ T cells was found significantly increased in SAT, gonadal and mesenteric VAT from infected mice. No difference was observed in the number of this T cell population in omental VAT, 7 days after i.p. challenge (Table 4). Similarly, the number of TCRβ$^+$NK1.1$^+$IFN-γ$^-$IL-10$^+$ and TCRβ$^+$NK1.1$^+$IFN-γ$^+$IL-10$^+$ T cells per g of adipose tissue did not differ between control and infected mice (data not shown).

Table 4. Number of TCRβ$^+$NK1.1$^+$IFN-γ$^+$IL-10$^-$ T cells in isolated adipose tissue SVF, detected in PBS i.p.-treated or *N. caninum* i.p.-infected mice with 1×10^7 tachyzoites, 7 days after challenge. Results are present as mean plus one standard deviation of three animals on each group. Statistical significant differences between groups is indicated (**P*<0,05; ***P*<0,01; ****P*<0,005).

No of TCRβ$^+$NK1.1$^+$ T cells/g AT x 10^3		SAT	Gonadal VAT	Omental VAT	Mesenteric VAT
IFN-γ$^+$IL-10$^-$	PBS	2,07±0,86	2,93±2,24	370,00±150,44	7,52±4,96
	NcT	21,53±3,93**	26,83±3,15***	156,00±58,64	30,870±10,80*

Together, these results suggest a role of NKT cells in IFN-γ production during the host immune response elicited by *N. caninum* infection.

4.4. IFN-γ and IL-10 production by TCRβ$^+$CD4$^+$ and TCRβ$^+$CD8$^+$ T cells in adipose tissue

T cells play an important role in host defense against *N. caninum* [35]. To assess if there is an expansion of CD4$^+$ and CD8$^+$ T cells in adipose tissue of i.p. infected mice, we analyzed these cell populations by flow cytometry (Figure 26).

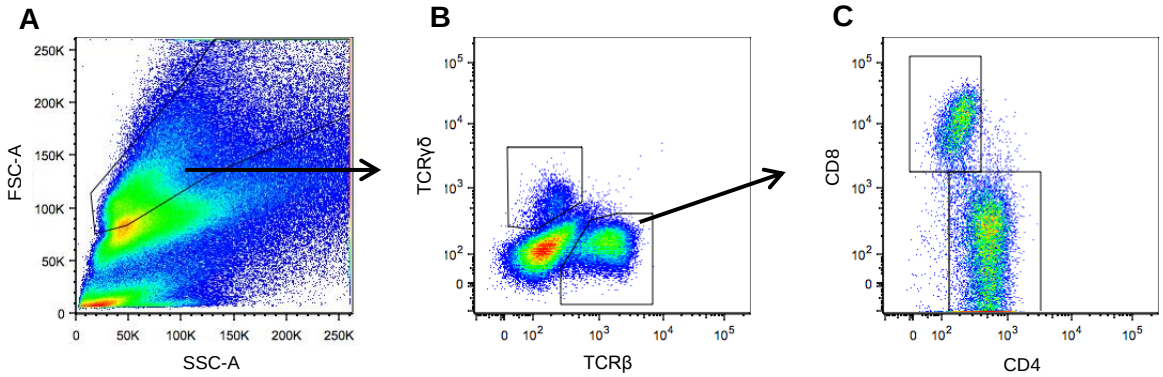

Figure 26. Representative dot plots of isolated SVF fraction from omental VAT of infected C57BL/6 mice. (A) Total leukocyte cells, (B) TCRβ$^+$TCRγδ$^-$ T cell population gated in A, (C) TCRβ$^+$ TCRγδ$^-$ T cells expressing CD4 and CD8.

Higher number of TCRβ$^+$CD4$^+$ (Figure 27A) and TCRβ$^+$CD8$^+$ (Figure 27B) T cells were found in the four types of the analyzed adipose tissue from infected mice when compared with controls, 7 days after i.p. challenge.

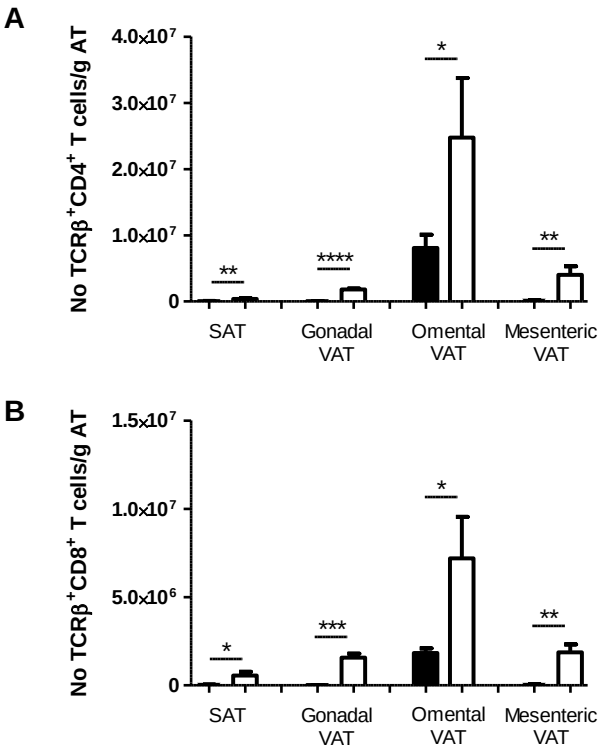

Figure 27. Number of (A) TCRβ$^+$CD4$^+$ and (B) TCRβ$^+$CD8$^+$ T cells in isolated adipose tissue SVF, detected in PBS i.p.-treated (■) or *N. caninum* i.p.-infected mice with 1×10^7 tachyzoites (□), 7 days after challenge. Bars represent mean plus one standard deviation of three animals on each group. Statistical significant differences between groups is indicated (*P<0,05; **P<0,01; ***P<0,005; ****P<0,0001).

The production of IFN-γ and IL-10 by CD4$^+$ and CD8$^+$ T cells was also evaluated by flow cytometry (Figure 28).

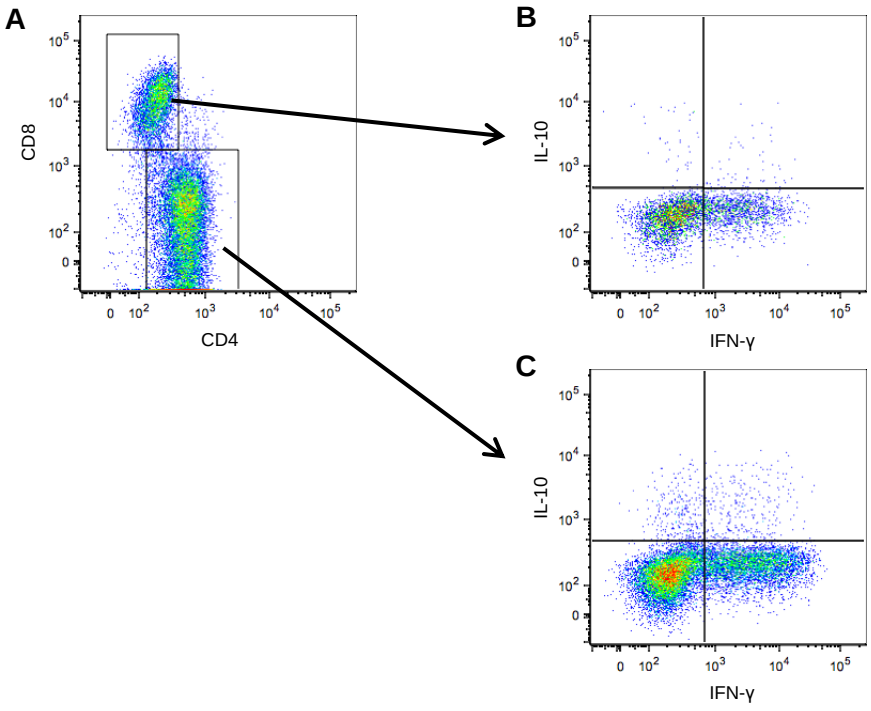

Figure 28. Representative dot plots of isolated SVF fraction from omental VAT of infected C57BL/6 mice. (A) CD8$^+$ and CD4$^+$ cells gated in TCRβ$^+$ T cells, (B) gated TCRβ$^+$CD8$^+$ and (C) TCRβ$^+$CD4$^+$ T cell population expressing IFN-γ and IL-10.

The frequency of $TCR\beta^+CD4^+IFN\text{-}\gamma^+IL\text{-}10^-$ cells was found significantly increased in SAT and mesenteric VAT from infected mice, where in gonadal and omental VAT there was no significant difference in the frequency of this cell populations (Figure 29A). The number of cells of this population increased in all types of analyzed adipose tissue from infected mice when compared to non-infected controls. The frequency of $TCR\beta^+CD4^+IFN\text{-}\gamma^-IL\text{-}10^+$ and $TCR\beta^+CD4^+IFN\text{-}\gamma^+IL\text{-}10^+$ cells was significantly increased in SAT from infected mice whereas no difference in the frequency of these cell populations between VAT of control and NcT challenged mice was observed (Figure 29B and C). Upon infection, an increased number of $TCR\beta^+CD4^+IFN\text{-}\gamma^-IL\text{-}10^+$ cells, in SAT, gonadal and omental VAT, and $TCR\beta^+CD4^+IFN\text{-}\gamma^+IL\text{-}10^+$ cells, in SAT, gonadal and mesenteric VAT, was observed. No such difference was found in $TCR\beta^+CD4^+IFN\text{-}\gamma^-IL\text{-}10^+$ and $TCR\beta^+CD4^+IFN\text{-}\gamma^+IL\text{-}10^+$ T cell numbers from mesenteric VAT and omental VAT, respectively (Table 5).

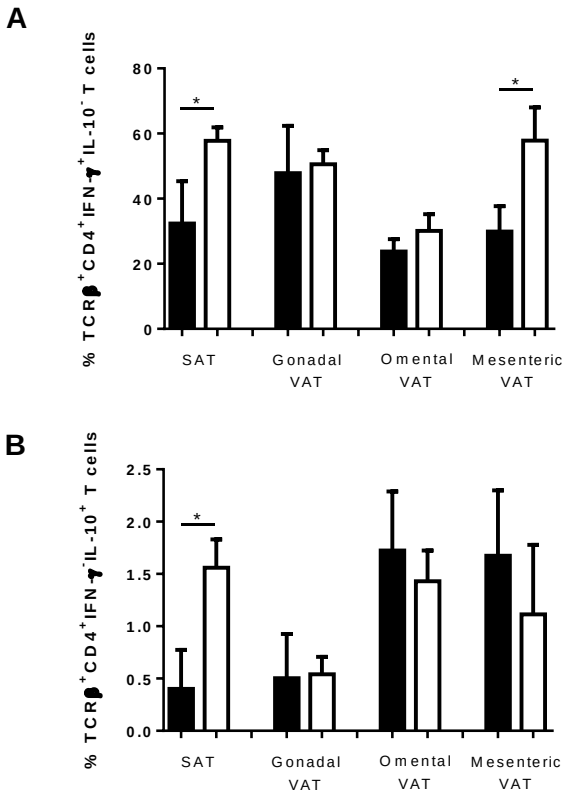

Continues in the following page

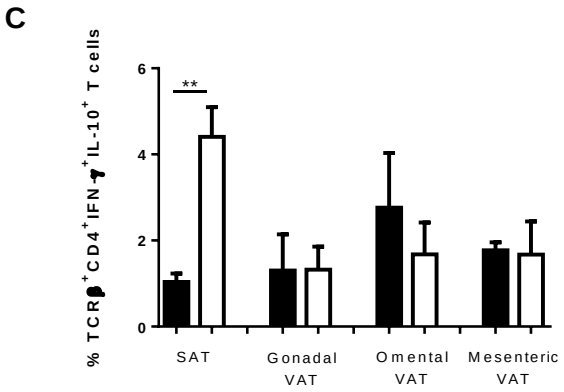

Figure 29. Frequency of (A) TCRβ$^+$CD4$^+$IFN-γ$^+$IL-10$^-$, (B) TCRβ$^+$CD4$^+$IFN-γ$^-$IL-10$^+$ and (C) TCRβ$^+$CD4$^+$IFN-γ$^+$IL-10$^+$ T cells in isolated adipose tissue SVF, detected in PBS i.p.-treated (■) or *N. caninum* i.p.-infected mice with 1×10^7 tachyzoites (□), 7 days after challenge. Bars represent mean plus one standard deviation of three animals on each group. Statistical significant differences between groups is indicated (**P*<0,05; ***P*<0,01).

Table 5. Number of TCRβ$^+$CD4$^+$IFN-γ$^+$IL-10$^-$, TCRβ$^+$CD4$^+$IFN-γ$^-$IL-10$^+$ and TCRβ$^+$ CD4$^+$IFN-γ$^+$IL-10$^+$ T cells in isolated adipose tissue SVF, detected in PBS i.p.-treated or *N. caninum* i.p.-infected mice with 1×10^7 tachyzoites, 7 days after challenge. Results are present as mean plus one standard deviation of three animals on each group. Statistical significant differences between groups is indicated (**P*<0,05; ***P*<0,01; ****P*<0,005).

No of TCRβ$^+$CD4$^+$ T cells/g AT x 10^3		**SAT**	**Gonadal VAT**	**Omental VAT**	**Mesenteric VAT**
IFN-γ$^+$IL-10$^-$	**PBS**	0,14±0,12	0,24±0,23	141,40±58,23	1,98±1,81
	NcT	5,92±1,62**	9,60±2,73***	337,00±71,86**	44,67±27,91*
IFN-γ$^-$IL-10$^+$	**PBS**	0,51±0,29	0,53±0,39	221,67±99,52	1,89±1,25
	NcT	17,10±6,48**	23,53±8,60**	388,33±177,39*	64,60±30,80
IFN-γ$^+$IL-10$^+$	**PBS**	8,94±7,27	4,93±2,25	653,67±229,62	8,60±4,99
	NcT	301,67±96,50*	498,67±29,33**	1857,00±768,66	645,67±201,70**

The frequency and number of single and double IFN-γ and IL-10 producers was also assessed in CD8$^+$ T cells from adipose tissue. As shown in figure 30A, the frequency of TCRβ$^+$CD8$^+$IFN-γ$^+$IL-10$^-$ cells was found to increase in SAT from infected mice whereas no significant difference was observed in the VAT of the NcT-challenged mice, comparatively to controls (Figure 30A). The number of cells of this population was found increased in SAT, gonadal and mesenteric VAT from infected mice comparatively with controls and did not suffer alterations in omental VAT from the same mice (Table 6). No differences were observed in the frequency of TCRβ$^+$CD8$^+$IFN-γ$^-$IL-10$^+$ T cells in adipose tissue after i.p. challenge (Figure 30B). SAT, gonadal and omental VAT did not show differences in the number of TCRβ$^+$CD8$^+$IFN-γ$^-$IL-10$^+$ T cells while an increase was observed in mesenteric VAT from infected mice (Table 6). Finally, the frequency and number of TCRβ$^+$CD8$^+$IFN-γ$^+$IL-10$^+$ T cells was higher in both SAT and mesenteric VAT from infected mice (Figure 30C and Table 6). No differences in frequency were observed in gonadal and mesenteric VAT (Figure 30C). However, gonadal VAT showed an increase

in the number of $CD8^+$ T cells IFN-γ and IL-10 double producers after infection. No such difference was observed in omental VAT from infected mice (Table 6).

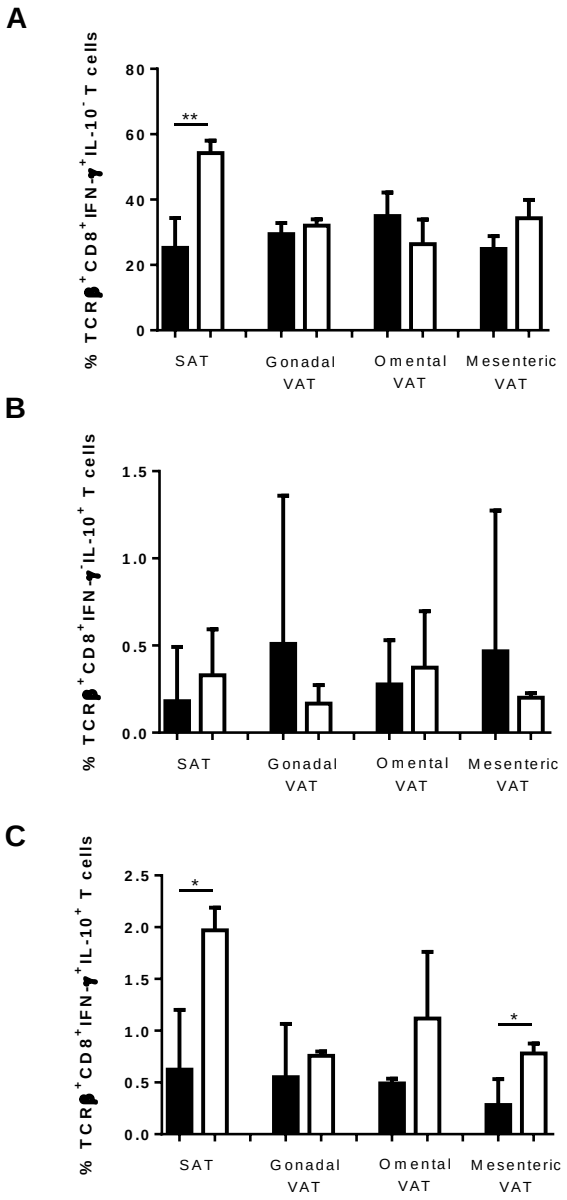

Figure 30. Frequency of (A) $TCR\beta^+CD8^+IFN\text{-}\gamma^+IL\text{-}10^-$, (B) $TCR\beta^+CD8^+IFN\text{-}\gamma^-IL\text{-}10^+$ and (C) $TCR\beta^+CD8^+IFN\text{-}\gamma^+IL\text{-}10^+$ T cells in isolated adipose tissue SVF, detected in PBS i.p.-treated (■) or *N. caninum* i.p.-infected mice with 1×10^7 tachyzoites (□), 7 days after challenge. Bars represent mean plus one standard deviation of three animals on each group. Statistical significant differences between groups is indicated (**P*<0,05; ***P*<0,01).

Table 6. Number of TCRβ$^+$CD8$^+$IFN-γ$^+$IL-10$^-$, TCRβ$^+$CD8$^+$IFN-γ$^-$IL-10$^+$ and TCRβ$^+$ CD8$^+$IFN-γ$^+$IL-10$^+$ T cells in isolated adipose tissue SVF, detected in PBS i.p.-treated or *N. caninum* i.p.-infected mice with 1×10^7 tachyzoites, 7 days after challenge. Results are present as mean plus one standard deviation of three animals on each group. Statistical significant differences between groups is indicated (**P*<0,05; ***P*<0,01; ****P*<0,005; *****P*<0,0001).

No of TCRβ$^+$CD8$^+$ T cells/g AT x 10^3		**SAT**	**Gonadal VAT**	**Omental VAT**	**Mesenteric VAT**
IFN-γ$^+$IL-10$^-$	**PBS**	8,94±7,23	4,93±2,25	653,67±229,62	8,60±4,99
	NcT	301,67±96,50**	498,67±50,80****	1857,00±768,66	645,67±201,70**
IFN-γ$^-$IL-10$^+$	**PBS**	0,030±0,053	0,09±0,14	4,64±4,18	0,00±0,00
	NcT	2,21±2,44	2,72±1,88	23,80±22,95	3,63±0,43***
IFN-γ$^+$IL-10$^+$	**PBS**	0,25±0,28	0,076±0,086	8,96±0,75	0,13±0,12
	NcT	11,29±5,22*	11,76±1,6***	78,90±58,32	14,73±0,54**

Altogether, these data suggest an activation of CD4$^+$ and CD8$^+$ T cells in adipose tissue of infected mice associated with a protective immune response due to a major IFN-γ production.

Discussion

Previous work from our team has shown that p40$^{-/-}$ C57BL/6 mice, which are lethally susceptible to neosporosis, presented a high colonization in mesenteric VAT after i.p. infection with *N. caninum* tachyzoites (Teixeira et al., unpublished results). Curiously, adipose tissue has been considered a reservoir for *M. tuberculosis* [71] and *T. cruzi* [74], where they can sequester fatty acids in order to survive. In this way, we hypothesized that adipose tissue could also be a site of *N. caninum* persistence within the host. Thus, our work aimed to detect the presence of the parasite in adipose tissue and characterize the host immune response in this tissue. In infected mice, tachyzoites have been detected in gonadal, mesenteric and omental VAT early after the parasitic infection, persisting in this place at least 7 days after infection. However, at this time point, only parasitic DNA could be detected by RT-PCR, which suggests a control of the infection in adipose tissue. Two months after infection, parasitic DNA was no longer detected in the analyzed adipose tissue depots, indicating that adipose tissue may not be a reservoir for *N. caninum*. Parasitic DNA and tachyzoites were also detected in the spleen, lungs and brain of infected mice, 7 days after infection. This observation is in agreement with a previous study in which parasite distribution kinetics was analyzed in *N. caninum* i.p.-challenged BALB/c mice [78].

Macrophages represent the most abundant immune cell population in adipose tissue, which may present different phenotypes [79]. When inflammatory signals in this tissue are low, macrophages are present in moderate quantities and exhibit the M2 phenotype, characterized by surface expression of CD206 and production of IL-10. The shift for a more marked inflammatory state, as occurs in obesity, with increased secretion of monocyte chemoattractants and pro-inflammatory signals, will lead to accumulation of macrophages displaying a M1 phenotype, characterized by CD11c surface expression and production of TNF-α, among other cytokines [63, 80]. A characterization of these two subpopulations in the course of neosporosis would be interesting, given that macrophages have a crucial role in the protective immune response against *N. caninum*, by increasing the production of NO, with subsequently killing of the parasite, and activating specific T lymphocytes [28, 29, 81]. So, the increased presence of macrophages in the adipose tissue depots observed in the infected mice may reflect their recruitment into this tissue, thus contributing to eliminate the parasite. The significant influx of macrophages into the adipose tissue was also observed in *T. cruzi* infected mice [74]. As adipocytes may release chemokines that lead to macrophage migration, it would be interesting to ascertain whether this could occur in the course of *N. caninum* infection. As it was

previously reported that in obese mice adipose tissue infiltrating monocytes will progressively undergo polarization towards an M1-like state [80], this further reinforces the importance of characterizing the function of macrophages found in the adipose tissue of *N. caninum*-infected mice. A result that must be highlighted is the increased number or macrophages observed in the IMAT of infected mice. Once skeletal muscle is known to be a place where parasite persists in a latent stage and we observed tachyzoites in skeletal muscle of mice 7 days upon infection by IHC analysis (data not shown), we may hypothesize that macrophages migrate to this tissue in response to infection.

The number of adipose tissue Treg cells is also variable according to the inflammatory microenvironment. In a non-inflammatory state such as found in lean mice, these cells are present in higher numbers than in obese mice and contribute for an M2 phenotype of macrophages, consistent with the role of Treg as a primary regulator of adipose tissue inflammation. A decrease in Treg numbers is associated with an inflammatory state and the accumulation of M1 macrophages in adipose tissue [66, 79, 82]. Treg cells also exhibit an important role in controlling exacerbated immune responses to infections, which may nevertheless result in enhanced pathogen persistence and survival [39, 83, 84]. An excessive activity of Treg cells contributes to immune suppression and can lead to an uncontrolled proliferation of the parasite, fatal to the host [85]. In this study, we observed an increase in the number of $CD4^+CD25^+Foxp3^-$ T cells and of $CD4^+CD25^+Foxp3^+$ T cells in the adipose tissue of infected mice, consistent with the observations made by others in the spleen of i.p.-infected mice, in the early stages of *N. caninum* infection [31, 41]. These results are indicative of an expansion or recruitment of effector T cells and Treg cells to adipose tissue of infected mice. The characterization of adipose tissue Treg cells in a later stage of infection with *N. caninum* would be worthwhile to perform.

NK cells were detected in high percentage in epididymal VAT pads of non-obese animals and demonstrated to be unaffected by the inflammatory state in adipose tissue [66]. In contrast, our data shows an increase in the number of NK cells in adipose tissue of infected mice, 7 days after infection. As previously reported, these cells display an important role in innate resistance to protozoan infections by inducing the lysis of target cells and by producing cytokines involved in the stimulation of other immune cells [25]. Although the frequency of IFN-γ-producing NK cells did not differ in adipose tissue depots between control and infected mice, the number of these cells was observed increased in VAT (gonadal and mesenteric) and SAT samples. Therefore, our data suggests that NK cells may be an important source of that pro-inflammatory cytokine in the adipose tissue. As *in vivo* studies showed an increased IFN-γ production at early stages of *N. caninum* infection [27], it would be interesting to determine whether adipose tissue NK cells may be

also early responders in murine neosporosis. Others have described, by performing *in vitro* studies, that IL-2-activated NK cells are IFN-γ-producers upon stimulation by *N. caninum*-infected bovine fibroblasts. These infected fibroblasts were also shown to have increased susceptibility to NK cell cytotoxicity mediated by a perforin-mediated mechanism [26]. Therefore it would be important to elucidate whether in the murine model the cytotoxic function of NK cells may contribute for the host defense against *N. caninum*.

The presence of cells in adipose tissue that exhibit characteristics of both innate and adaptive immunity, as γδ and NK T cells, has been documented [86]. γδ T cells were found in higher proportions at epididymal VAT depots that showed an inflammatory state [55]. Their function in infectious diseases, including in *N. caninum* infection, is still largely unknown. However, it has been shown that these cells played a host-protective role against *Eimeria vermiformis* activating components of the innate immune system, such as NK cells [87], and as IFN-γ-producers in early immune responses against *T. gondii* [88] and *Listeria monocytogenes* [89]. Given the increased number of IFN-γ-producing TCRγδ$^+$ T cells found in adipose tissue samples from infected mice, we may hypothesize a role of this cell population in host resistance against *N. caninum* infection.

NKT cells, are enriched in non-obese mouse adipose tissue and their number increases in the course of adipose tissue inflammation [90]. NKT cells are known to produce large amounts of Th1 or Th2 cytokines following stimulation, influencing macrophage phenotypes in both beneficial and harmful ways [62, 91]. As we observed an increase in the number of IFN-γ-producing TCRβ$^+$NK1.1$^+$ T cells, in the adipose tissue, we may hypothesize that, upon *N. caninum* infection, NKT cells induced a M1 phenotype by IFN-γ secretion and amplified a pro-inflammatory status of adipose tissue by inducing a Th1 response [66, 92]. In omental VAT from infected mice there was a decrease in NKT cell number. A possible explanation for this observation may reside in apoptosis due to TCR-activation-induced cell death, that followed IFN-γ production, as reported in a study of α-galactosylceramide administration [93].

An inflammatory microenvironment in adipose tissue induces accumulation of CD8$^+$ T cells that will activate and recruit M1 macrophages, which coincides with a reduction in Treg cell numbers and leads to the activation of Th1 CD4$^+$ T cells [66, 94]. Adipose tissue macrophages promote the proliferation of IFN-γ-producing CD4$^+$ T cells through antigenic presentation by MHC class II [94]. The increased number of CD4$^+$ T cells observed in fat depots from infected mice may be due to macrophage-drive activation of those cells. Also, CD8$^+$ T cells were found in higher number in adipose tissue of infected mice. Even though CD8$^+$ T cells function is not crucial, though necessary, for protection against *N. caninum*, as compared with CD4$^+$ T cells, this cell population was described as early IFN-γ-producers upon *N. caninum* infection [27, 31, 35]. In this regard,

IFN-γ production by $CD8^+$ T cells early in infection would be interesting to evaluate and compare with production by $CD4^+$ T cells since $CD8^+IFN\text{-}\gamma^+$ T cells were found in adipose tissue of infected mice, 7 days after infection.

After an infection, the development of an immune response by the host is of extreme importance, determining the protection or susceptibility to the pathogen. NcT induces an early DC activation with IL-12 production, which is essential for T cell differentiation towards a Th1 immune phenotype [30-32, 36]. Considering that we observed an increase in the number of $CD4^+$ T cells in the analyzed adipose tissue, it would be interesting to study the DC population and IL-12 production, by these and other cells, in this tissue. Nevertheless, our results strongly indicate that T cells were differentiated towards the Th1 phenotype, given the higher number of IFN-γ-producing $CD4^+$ T cells in adipose tissue of infected mice.

$CD4^+$ and $CD8^+$ effector T cells were found to produce IL-10 in the adipose tissue upon *N. caninum* infection. The majority of these IL-10-producing $CD4^+$ T cells probably correspond to Treg cells, which were seen to increase in number at this place [67] and were described as IL-10-producers in several infections [39, 95]. On the other hand, $CD8^+$ T cells that produce this anti-inflammatory cytokine could be CD8 Treg cells, generated in the presence of IL-12, or activated CD8 effector T cells, as was described in influenza virus infection [96, 97]. An interesting finding was the double production of IFN-γ and IL-10 by $CD4^+$ and $CD8^+$ T cells. $CD4^+$ T cells double producers have been described in *T. cruzi* [98] and *T. gond*ii [99] infection. This population is able to prevent collateral immune damage and is required for maintaining a chronic, non-resolving infection status [100]. Double production of IFN-γ and IL-10 by $CD8^+$ T cells has been reported in *T. cruzi* [101] and in influenza virus infection [97].

The observed differences in cell populations among the four analyzed adipose tissue depots are not surprising and may be explained by the unique immune profile and different cellular composition, previously described for SAT and several VAT pads [86, 102]. However, the differences observed in cell populations and cytokine production between SAT from control and infected mice were not expected. Once *N. caninum* was only detected in SAT from one mouse, these differences are hardly explained by the presence of the parasite. Nevertheless, we may not exclude that APC containing the parasite can migrate to SAT and induce an immune response, early after infection. As far as we know, this is the first study of the host immune response upon infection in the several adipose tissue depots, in particular in SAT and IMAT.

Conclusion

In conclusion, the present study has demonstrated that *N. caninum* tachyzoites colonize several depots of adipose tissue from C57BL/6 mice, persisting here at least for 7 days after i.p. infection. However it is unlikely that this tissue may be a long-term reservoir for *N. caninum*.

Our work is the first addressing the immune response to neosporosis in the adipose tissue. The presence of tachyzoites inside of what seems to be macrophages and the increased number of those cells in adipose tissue suggests a protective role played by macrophages therein. The difference in macrophage numbers was accompanied by the increased presence of $CD4^+$ and $CD8^+$ effector T cells and Treg cells. $CD4^+$ T cells appeared to be differentiated towards the Th1 phenotype given the higher number of IFN-γ-producing cells. Additionally, $CD8^+$ T cells and TCRγδ, NK and NKT cells were found to produce this pro-inflammatory cytokine, indicating a possible protective role of all these cellular subsets early after *N. caninum* infection. Although we have not assessed the production of IL-10 by Treg cells, this cytokine was detected in adipose tissue. Interestingly, $CD4^+$ and $CD8^+$ T cells were identified as IFN-γ and IL-10 double producers. It remains to be elucidated whether they may have a role in controlling excessive inflammation and/or immune evasion by *N. caninum*.

More studies are needed in order to assess the importance of each population analyzed in the adipose tissue and their contribution to a protective or susceptible host immune response in the course of a *N. caninum* infection.

Future perspectives

In this work we have tried to identify the precise location of *N. caninum* in adipose tissue collected from infected mice, namely if this parasite could be found inside adipocytes as described for other protozoan parasites [74]. However, due to technical problems with the immunofluorescence analysis, we were not able to draw any conclusion in this regard. Co-cultures of NcT and adipocytes differentiated *in vitro* from the pre-adipocyte cell line 3T3-L1 could shed some light into this subject.

A marked increase in adipose tissue macrophages after NcT challenge was observed. Since adipose tissue macrophages phenotype differs according to the local pro or anti-inflammatory state, it would be interesting to characterize the phenotype of macrophages found in the adipose tissue upon *N. caninum* infection. This could be accomplished by flow cytometric analysis of the surface antigens $F4/80^{+}CD11c^{+}$ (M1) and $F4/80^{+}CD206^{+}$ (M2) or by evaluation of cytokines associated to each phenotype, TNF-α, IL-6 and IL-12 are produced by M1 and IL-10 is produced by M2 macrophages.

Innate and adaptive immune cells are involved in the host immune response against *N. caninum* infection. Splenic and MLN DC were found to be early producers of IL-12 in *N. caninum*-infected mice [30, 31] and *in vitro* studies have shown that DC exposed to this parasite stimulate IFN-γ-secretion [81]. Since a marked increase in the number of adipose tissue T cells producing IFN-γ was observed in *N. caninum* infected mice it would be interesting to analyze whether DC are present in this tissue and their respective function, assessing in particular their production of IL-12 at early time points after infection.

Concerning cytokine production in response to *N. caninum*, this work focused only in IFN-γ and IL-10. However, the presence of IL-4 has also been detected in mice infected with *N. caninum* and a high IL-4:IFN-γ ratio has been associated with host susceptibility to neosporosis [37]. Therefore, it would be interesting to assess IL-4 production by T cells in the different types of adipose tissue depots to evaluate if a bias towards either a Th1 or Th2 response could occur.

References

1. Bjerkas, I., Mohn, S.F., and Presthus, J. (1984) Unidentified cyst-forming sporozoon causing encephalomyelitis and myositis in dogs. *Z Parasitenkd*, **70**, 271-274.
2. Parish, S.M., Maag-Miller, L., Besser, T.E., Weidner, J.P., McElwain, T., Knowles, D.P., and Leathers, C.W. (1987) Myelitis associated with protozoal infection in newborn calves. *J Am Vet Med Assoc*, **191**, 1599-1600.
3. O'Toole, D. and Jeffrey, M. (1987) Congenital sporozoan encephalomyelitis in a calf. *Vet Rec*, **121**, 563-566.
4. Dubey, J.P., Carpenter, J.L., Speer, C.A., Topper, M.J., and Uggla, A. (1988) Newly recognized fatal protozoan disease of dogs. *J Am Vet Med Assoc*, **192**, 1269-1285.
5. Dubey, J.P., Jenkins, M.C., Rajendran, C., Miska, K., Ferreira, L.R., Martins, J., Kwok, O.C., and Choudhary, S. (2011) Gray wolf (*Canis lupus*) is a natural definitive host for *Neospora caninum. Vet Parasitol*, **181**, 382-387.
6. Dubey, J.P. and Schares, G. (2011) Neosporosis in animals-the last five years. *Vet Parasitol*, **180**, 90-108.
7. McCann, C.M., Vyse, A.J., Salmon, R.L., Thomas, D., Williams, D.J., McGarry, J.W., Pebody, R., and Trees, A.J. (2008) Lack of serologic evidence of *Neospora caninum* in humans, England. *Emerg Infect Dis*, **14**, 978-980.
8. Barr, B.C., Conrad, P.A., Sverlow, K.W., Tarantal, A.F., and Hendrickx, A.G. (1994) Experimental fetal and transplacental *Neospora* infection in the nonhuman primate. *Lab Invest*, **71**, 236-242.
9. Lobato, J., Silva, D.A., Mineo, T.W., Amaral, J.D., Segundo, G.R., Costa-Cruz, J.M., Ferreira, M.S., Borges, A.S., and Mineo, J.R. (2006) Detection of immunoglobulin G antibodies to *Neospora caninum* in humans: high seropositivity rates in patients who are infected by human immunodeficiency virus or have neurological disorders. *Clin Vaccine Immunol*, **13**, 84-89.
10. Goodswen, S.J., Kennedy, P.J., and Ellis, J.T. (2013) A review of the infection, genetics, and evolution of *Neospora caninum*: from the past to the present. *Infect Genet Evol*, **13**, 133-150.
11. Almeria, S. and Lopez-Gatius, F. (2013) Bovine neosporosis: Clinical and practical aspects. *Res Vet Sci*, **95**, 303-309.
12. Dubey, J.P. (2003) Review of *Neospora caninum* and neosporosis in animals. *Korean J Parasitol*, **41**, 1-16.

13. Dubey, J.P., Barr, B.C., Barta, J.R., Bjerkas, I., Bjorkman, C., Blagburn, B.L., Bowman, D.D., Buxton, D., Ellis, J.T., Gottstein, B., Hemphill, A., Hill, D.E., Howe, D.K., Jenkins, M.C., Kobayashi, Y., Koudela, B., Marsh, A.E., Mattsson, J.G., McAllister, M.M., Modry, D., Omata, Y., Sibley, L.D., Speer, C.A., Trees, A.J., Uggla, A., Upton, S.J., Williams, D.J., and Lindsay, D.S. (2002) Redescription of *Neospora caninum* and its differentiation from related coccidia. *Int J Parasitol*, **32**, 929-946.
14. Dubey, J.P., Koestner, A., and Piper, R.C. (1990) Repeated transplacental transmission of *Neospora caninum* in dogs. *J Am Vet Med Assoc*, **197**, 857-860.
15. Dubey, J.P. and Lindsay, D.S. (1996) A review of *Neospora caninum* and neosporosis. *Vet Parasitol*, **67**, 1-59.
16. Eastick, F.A. and Elsheikha, H.M. (2010) Stress-driven stage transformation of *Neospora caninum. Parasitol Res*, **106**, 1009-1014.
17. Haddad, J.P., Dohoo, I.R., and VanLeewen, J.A. (2005) A review of *Neospora caninum* in dairy and beef cattle-a Canadian perspective. *Can Vet J*, **46**, 230-243.
18. Reichel, M.P., Ellis, J.T., and Dubey, J.P. (2007) Neosporosis and hammondiosis in dogs. *J Small Anim Pract*, **48**, 308-312.
19. Hemphill, A., Vonlaufen, N., and Naguleswaran, A. (2006) Cellular and immunological basis of the host-parasite relationship during infection with *Neospora caninum. Parasitology*, **133**, 261-278.
20. Dubey, J.P., Buxton, D., and Wouda, W. (2006) Pathogenesis of bovine neosporosis. *J Comp Pathol*, **134**, 267-289.
21. Dubey, J.P., Schares, G., and Ortega-Mora, L.M. (2007) Epidemiology and control of neosporosis and *Neospora caninum. Clin Microbiol Rev*, **20**, 323-367.
22. Williams, D.J., Guy, C.S., McGarry, J.W., Guy, F., Tasker, L., Smith, R.F., MacEachern, K., Cripps, P.J., Kelly, D.F., and Trees, A.J. (2000) *Neospora caninum*-associated abortion in cattle: the time of experimentally-induced parasitaemia during gestation determines foetal survival. *Parasitology*, **121 (Pt 4)**, 347-358.
23. Reichel, M.P., Alejandra Ayanegui-Alcerreca, M., Gondim, L.F., and Ellis, J.T. (2013) What is the global economic impact of *Neospora caninum* in cattle - the billion dollar question. *Int J Parasitol*, **43**, 133-142.
24. Dubey, J.P. and Schares, G. (2006) Diagnosis of bovine neosporosis. *Vet Parasitol*, **140**, 1-34.
25. Scharton-Kersten, T.M. and Sher, A. (1997) Role of natural killer cells in innate resistance to protozoan infections. *Curr Opin Immunol*, **9**, 44-51.

26. Boysen, P., Klevar, S., Olsen, I., and Storset, A.K. (2006) The protozoan *Neospora caninum* directly triggers bovine NK cells to produce gamma interferon and to kill infected fibroblasts*. Infect Immun*, **74**, 953-960.

27. Klevar, S., Kulberg, S., Boysen, P., Storset, A.K., Moldal, T., Bjorkman, C., and Olsen, I. (2007) Natural killer cells act as early responders in an experimental infection with *Neospora caninum* in calves*. Int J Parasitol*, **37**, 329-339.

28. Tanaka, T., Nagasawa, H., Fujisaki, K., Suzuki, N., and Mikami, T. (2000) Growth-inhibitory effects of interferon-gamma on *Neospora caninum* in murine macrophages by a nitric oxide mechanism*. Parasitol Res*, **86**, 768-771.

29. Nishikawa, Y., Tragoolpua, K., Inoue, N., Makala, L., Nagasawa, H., Otsuka, H., and Mikami, T. (2001) In the absence of endogenous gamma interferon, mice acutely infected with *Neospora caninum* succumb to a lethal immune response characterized by inactivation of peritoneal macrophages*. Clin Diagn Lab Immunol*, **8**, 811-816.

30. Teixeira, L., Botelho, A.S., Mesquita, S.D., Correia, A., Cerca, F., Costa, R., Sampaio, P., Castro, A.G., and Vilanova, M. (2010) Plasmacytoid and conventional dendritic cells are early producers of IL-12 in *Neospora caninum*-infected mice*. Immunol Cell Biol*, **88**, 79-86.

31. Correia, A., Ferreirinha, P., Costa, A.A., Dias, J., Melo, J., Costa, R., Ribeiro, A., Faustino, A., Teixeira, L., Rocha, A., and Vilanova, M. (2013) Mucosal and systemic T cell response in mice intragastrically infected with *Neospora caninum* tachyzoites*. Vet Res*, **44**, 69.

32. Baszler, T.V., Long, M.T., McElwain, T.F., and Mathison, B.A. (1999) Interferon-gamma and interleukin-12 mediate protection to acute *Neospora caninum* infection in BALB/c mice*. Int J Parasitol*, **29**, 1635-1646.

33. Khan, I.A., Schwartzman, J.D., Fonseka, S., and Kasper, L.H. (1997) *Neospora caninum*: role for immune cytokines in host immunity*. Exp Parasitol*, **85**, 24-34.

34. Long, M.T., Baszler, T.V., and Mathison, B.A. (1998) Comparison of intracerebral parasite load, lesion development, and systemic cytokines in mouse strains infected with *Neospora caninum. J Parasitol*, **84**, 316-320.

35. Tanaka, T., Hamada, T., Inoue, N., Nagasawa, H., Fujisaki, K., Suzuki, N., and Mikami, T. (2000) The role of CD4(+) or CD8(+) T cells in the protective immune response of BALB/c mice to *Neospora caninum* infection*. Vet Parasitol*, **90**, 183-191.

36. Botelho, A.S., Teixeira, L., Correia-da-Costa, J.M., Faustino, A.M., Castro, A.G., and Vilanova, M. (2007) *Neospora caninum*: high susceptibility to the parasite in C57BL/10ScCr mice*. Exp Parasitol*, **115**, 68-75.

37. Baszler, T.V., McElwain, T.F., and Mathison, B.A. (2000) Immunization of BALB/c mice with killed *Neospora caninum* tachyzoite antigen induces a type 2 immune response and exacerbates encephalitis and neurological disease. *Clin Diagn Lab Immunol*, **7**, 893-898.

38. Rowe, J.H., Ertelt, J.M., and Way, S.S. (2012) Foxp3(+) regulatory T cells, immune stimulation and host defence against infection. *Immunology*, **136**, 1-10.

39. Flores-Garcia, Y., Rosales-Encina, J.L., Rosales-Garcia, V.H., Satoskar, A.R., and Talamas-Rohana, P. (2013) CD4+ CD25+ FOXP3+ Treg cells induced by rSSP4 derived from *T. cruzi* amastigotes increase parasitemia in an experimental Chagas disease model. *Biomed Res Int*, **2013**, 632436.

40. Snapper, C.M. and Paul, W.E. (1987) Interferon-gamma and B cell stimulatory factor-1 reciprocally regulate Ig isotype production. *Science*, **236**, 944-947.

41. Teixeira, L., Botelho, A.S., Batista, A.R., Meireles, C.S., Ribeiro, A., Domingues, H.S., Correia Da Costa, J.M., Castro, A.G., Faustino, A.M., and Vilanova, M. (2007) Analysis of the immune response to *Neospora caninum* in a model of intragastric infection in mice. *Parasite Immunol*, **29**, 23-36.

42. Hemphill, A., Debache, K., Monney, T., Schorer, M., Guionaud, C., Alaeddine, F., Mueller, N., and Mueller, J. (2013) Proteins mediating the *Neospora caninum*-host cell interaction as targets for vaccination. *Front Biosci (Elite Ed)*, **5**, 23-36.

43. Innes, E.A., Andrianarivo, A.G., Bjorkman, C., Williams, D.J., and Conrad, P.A. (2002) Immune responses to *Neospora caninum* and prospects for vaccination. *Trends Parasitol*, **18**, 497-504.

44. Reichel, M.P. and Ellis, J.T. (2009) *Neospora caninum*--how close are we to development of an efficacious vaccine that prevents abortion in cattle? *Int J Parasitol*, **39**, 1173-1187.

45. Williams, D.J., Guy, C.S., Smith, R.F., Ellis, J., Bjorkman, C., Reichel, M.P., and Trees, A.J. (2007) Immunization of cattle with live tachyzoites of *Neospora caninum* confers protection against fetal death. *Infect Immun*, **75**, 1343-1348.

46. Cho, J.H., Chung, W.S., Song, K.J., Na, B.K., Kang, S.W., Song, C.Y., and Kim, T.S. (2005) Protective efficacy of vaccination with *Neospora caninum* multiple recombinant antigens against experimental Neospora caninum infection. *Korean J Parasitol*, **43**, 19-25.

47. Pinitkiatisakul, S., Mattsson, J.G., Wikman, M., Friedman, M., Bengtsson, K.L., Stahl, S., and Lunden, A. (2005) Immunisation of mice against neosporosis with recombinant NcSRS2 iscoms. *Vet Parasitol*, **129**, 25-34.

48. Nishikawa, Y., Xuan, X., Nagasawa, H., Igarashi, I., Fujisaki, K., Otsuka, H., and Mikami, T. (2001) Prevention of vertical transmission of *Neospora caninum* in

BALB/c mice by recombinant vaccinia virus carrying NcSRS2 gene. *Vaccine*, **19**, 1710-1716.

49. Nishikawa, Y., Inoue, N., Xuan, X., Nagasawa, H., Igarashi, I., Fujisaki, K., Otsuka, H., and Mikami, T. (2001) Protective efficacy of vaccination by recombinant vaccinia virus against *Neospora caninum* infection. *Vaccine*, **19**, 1381-1390.
50. Debache, K. and Hemphill, A. (2013) Differential effects of intranasal vaccination with recombinant NcPDI in different mouse models of *Neospora caninum* infection. *Parasite Immunol*, **35**, 11-20.
51. Weston, J.F., Heuer, C., and Williamson, N.B. (2012) Efficacy of a *Neospora caninum* killed tachyzoite vaccine in preventing abortion and vertical transmission in dairy cattle. *Prev Vet Med*, **103**, 136-144.
52. Schaffler, A. and Scholmerich, J. (2010) Innate immunity and adipose tissue biology. *Trends Immunol*, **31**, 228-235.
53. Gil, A., Olza, J., Gil-Campos, M., Gomez-Llorente, C., and Aguilera, C.M. (2011) Is adipose tissue metabolically different at different sites? *Int J Pediatr Obes*, **6 Suppl 1**, 13-20.
54. Wronska, A. and Kmiec, Z. (2012) Structural and biochemical characteristics of various white adipose tissue depots. *Acta Physiol (Oxf)*, **205**, 194-208.
55. Caspar-Bauguil, S., Cousin, B., Bour, S., Casteilla, L., Penicaud, L., and Carpene, C. (2009) Adipose tissue lymphocytes: types and roles. *J Physiol Biochem*, **65**, 423-436.
56. Smith, S.B., Kawachi, H., Choi, C.B., Choi, C.W., Wu, G., and Sawyer, J.E. (2009) Cellular regulation of bovine intramuscular adipose tissue development and composition. *J Anim Sci*, **87**, E72-82.
57. Pond, C.M. (2005) Adipose tissue and the immune system. *Prostaglandins Leukot Essent Fatty Acids*, **73**, 17-30.
58. Desruisseaux, M.S., Nagajyothi, Trujillo, M.E., Tanowitz, H.B., and Scherer, P.E. (2007) Adipocyte, adipose tissue, and infectious disease. *Infect Immun*, **75**, 1066-1078.
59. Kaminski, D.A. and Randall, T.D. (2010) Adaptive immunity and adipose tissue biology. *Trends Immunol*, **31**, 384-390.
60. Platell, C., Cooper, D., Papadimitriou, J.M., and Hall, J.C. (2000) The omentum. *World J Gastroenterol*, **6**, 169-176.
61. Schipper, H.S., Prakken, B., Kalkhoven, E., and Boes, M. (2012) Adipose tissue-resident immune cells: key players in immunometabolism. *Trends Endocrinol Metab*, **23**, 407-415.

62. Mathis, D. (2013) Immunological Goings-on in Visceral Adipose Tissue. *Cell Metab*, **17**, 851-859.
63. Lumeng, C.N., Bodzin, J.L., and Saltiel, A.R. (2007) Obesity induces a phenotypic switch in adipose tissue macrophage polarization. *J Clin Invest*, **117**, 175-184.
64. Suganami, T. and Ogawa, Y. (2010) Adipose tissue macrophages: their role in adipose tissue remodeling. *J Leukoc Biol*, **88**, 33-39.
65. Wu, D., Molofsky, A.B., Liang, H.E., Ricardo-Gonzalez, R.R., Jouihan, H.A., Bando, J.K., Chawla, A., and Locksley, R.M. (2011) Eosinophils sustain adipose alternatively activated macrophages associated with glucose homeostasis. *Science*, **332**, 243-247.
66. Nishimura, S., Manabe, I., Nagasaki, M., Eto, K., Yamashita, H., Ohsugi, M., Otsu, M., Hara, K., Ueki, K., Sugiura, S., Yoshimura, K., Kadowaki, T., and Nagai, R. (2009) CD8+ effector T cells contribute to macrophage recruitment and adipose tissue inflammation in obesity. *Nat Med*, **15**, 914-920.
67. Feuerer, M., Herrero, L., Cipolletta, D., Naaz, A., Wong, J., Nayer, A., Lee, J., Goldfine, A.B., Benoist, C., Shoelson, S., and Mathis, D. (2009) Lean, but not obese, fat is enriched for a unique population of regulatory T cells that affect metabolic parameters. *Nat Med*, **15**, 930-939.
68. Zuniga, L.A., Shen, W.J., Joyce-Shaikh, B., Pyatnova, E.A., Richards, A.G., Thom, C., Andrade, S.M., Cua, D.J., Kraemer, F.B., and Butcher, E.C. (2010) IL-17 regulates adipogenesis, glucose homeostasis, and obesity. *J Immunol*, **185**, 6947-6959.
69. Rakhshandehroo, M., Kalkhoven, E., and Boes, M. (2013) Invariant natural killer T cells in adipose tissue: novel regulators of immune-mediated metabolic disease. *Cell Mol Life Sci*.
70. Gray, K.S., Collins, C.M., and Speck, S.H. (2012) Characterization of omental immune aggregates during establishment of a latent gammaherpesvirus infection. *PLoS One*, **7**, e43196.
71. Neyrolles, O., Hernandez-Pando, R., Pietri-Rouxel, F., Fornes, P., Tailleux, L., Barrios Payan, J.A., Pivert, E., Bordat, Y., Aguilar, D., Prevost, M.C., Petit, C., and Gicquel, B. (2006) Is adipose tissue a place for *Mycobacterium tuberculosis* persistence? *PLoS One*, **1**, e43.
72. Garton, N.J., Christensen, H., Minnikin, D.E., Adegbola, R.A., and Barer, M.R. (2002) Intracellular lipophilic inclusions of mycobacteria in vitro and in sputum. *Microbiology*, **148**, 2951-2958.
73. Combs, T.P., Nagajyothi, Mukherjee, S., de Almeida, C.J., Jelicks, L.A., Schubert, W., Lin, Y., Jayabalan, D.S., Zhao, D., Braunstein, V.L., Landskroner-Eiger, S.,

Cordero, A., Factor, S.M., Weiss, L.M., Lisanti, M.P., Tanowitz, H.B., and Scherer, P.E. (2005) The adipocyte as an important target cell for *Trypanosoma cruzi* infection*. J Biol Chem*, **280**, 24085-24094.

74. Nagajyothi, F., Desruisseaux, M.S., Machado, F.S., Upadhya, R., Zhao, D., Schwartz, G.J., Teixeira, M.M., Albanese, C., Lisanti, M.P., Chua, S.C., Jr., Weiss, L.M., Scherer, P.E., and Tanowitz, H.B. (2012) Response of adipose tissue to early infection with *Trypanosoma cruzi* (Brazil strain)*. J Infect Dis*, **205**, 830-840.
75. Mosser, D.M. and Edwards, J.P. (2008) Exploring the full spectrum of macrophage activation*. Nat Rev Immunol*, **8**, 958-969.
76. Su, D., Shen, M., Li, X., and Sun, L. (2013) Roles of gammadelta T cells in the pathogenesis of autoimmune diseases*. Clin Dev Immunol*, **2013**, 985753.
77. Zakka, L.R., Fradkov, E., Keskin, D.B., Tabansky, I., Stern, J.N., and Ahmed, A.R. (2012) The role of natural killer cells in autoimmune blistering diseases*. Autoimmunity*, **45**, 44-54.
78. Collantes-Fernandez, E., Lopez-Perez, I., Alvarez-Garcia, G., and Ortega-Mora, L.M. (2006) Temporal distribution and parasite load kinetics in blood and tissues during *Neospora caninum* infection in mice*. Infect Immun*, **74**, 2491-2494.
79. Ferrante, A.W., Jr. (2013) The immune cells in adipose tissue*. Diabetes Obes Metab*, **15 Suppl 3**, 34-38.
80. Oh, D.Y., Morinaga, H., Talukdar, S., Bae, E.J., and Olefsky, J.M. (2012) Increased macrophage migration into adipose tissue in obese mice*. Diabetes*, **61**, 346-354.
81. Dion, S., Germon, S., Guiton, R., Ducournau, C., and Dimier-Poisson, I. (2011) Functional activation of T cells by dendritic cells and macrophages exposed to the intracellular parasite *Neospora caninum. Int J Parasitol*, **41**, 685-695.
82. Cipolletta, D., Kolodin, D., Benoist, C., and Mathis, D. (2011) Tissular T(regs): a unique population of adipose-tissue-resident Foxp3+CD4+ T cells that impacts organismal metabolism*. Semin Immunol*, **23**, 431-437.
83. Belkaid, Y. and Tarbell, K. (2009) Regulatory T cells in the control of host-microorganism interactions (*)*. Annu Rev Immunol*, **27**, 551-589.
84. Ji, J., Masterson, J., Sun, J., and Soong, L. (2005) CD4+CD25+ regulatory T cells restrain pathogenic responses during *Leishmania amazonensis* infection*. J Immunol*, **174**, 7147-7153.
85. Hisaeda, H., Maekawa, Y., Iwakawa, D., Okada, H., Himeno, K., Kishihara, K., Tsukumo, S., and Yasutomo, K. (2004) Escape of malaria parasites from host immunity requires CD4+ CD25+ regulatory T cells*. Nat Med*, **10**, 29-30.

86. Caspar-Bauguil, S., Cousin, B., Galinier, A., Segafredo, C., Nibbelink, M., Andre, M., Casteilla, L., and Penicaud, L. (2005) Adipose tissues as an ancestral immune organ: site-specific change in obesity. *FEBS Lett*, **579**, 3487-3492.

87. Smith, A.L. and Hayday, A.C. (2000) An αβ T-cell-independent immunoprotective response towards gut coccidia is supported by γδ cells. *Immunology*, **101**, 325-332.

88. Hisaeda, H., Sakai, T., Maekawa, Y., Ishikawa, H., Yasutomo, K., and Himeno, K. (1996) Mechanisms of HSP65 expression induced by gamma delta T cells in murine *Toxoplasma gondii* infection. *Pathobiology*, **64**, 198-203.

89. Hiromatsu, K., Yoshikai, Y., Matsuzaki, G., Ohga, S., Muramori, K., Matsumoto, K., Bluestone, J.A., and Nomoto, K. (1992) A protective role of gamma/delta T cells in primary infection with *Listeria monocytogenes* in mice. *J Exp Med*, **175**, 49-56.

90. Mantell, B.S., Stefanovic-Racic, M., Yang, X., Dedousis, N., Sipula, I.J., and O'Doherty, R.M. (2011) Mice lacking NKT cells but with a complete complement of CD8+ T-cells are not protected against the metabolic abnormalities of diet-induced obesity. *PLoS One*, **6**, e19831.

91. Schipper, H.S., Rakhshandehroo, M., van de Graaf, S.F., Venken, K., Koppen, A., Stienstra, R., Prop, S., Meerding, J., Hamers, N., Besra, G., Boon, L., Nieuwenhuis, E.E., Elewaut, D., Prakken, B., Kersten, S., Boes, M., and Kalkhoven, E. (2012) Natural killer T cells in adipose tissue prevent insulin resistance. *J Clin Invest*, **122**, 3343-3354.

92. Winer, S., Chan, Y., Paltser, G., Truong, D., Tsui, H., Bahrami, J., Dorfman, R., Wang, Y., Zielenski, J., Mastronardi, F., Maezawa, Y., Drucker, D.J., Engleman, E., Winer, D., and Dosch, H.M. (2009) Normalization of obesity-associated insulin resistance through immunotherapy. *Nat Med*, **15**, 921-929.

93. Hayakawa, Y., Takeda, K., Yagita, H., Kakuta, S., Iwakura, Y., Van Kaer, L., Saiki, I., and Okumura, K. (2001) Critical contribution of IFN-gamma and NK cells, but not perforin-mediated cytotoxicity, to anti-metastatic effect of alpha-galactosylceramide. *Eur J Immunol*, **31**, 1720-1727.

94. Morris, D.L., Cho, K.W., Delproposto, J.L., Oatmen, K.E., Geletka, L.M., Martinez-Santibanez, G., Singer, K., and Lumeng, C.N. (2013) Adipose tissue macrophages function as antigen-presenting cells and regulate adipose tissue CD4+ T cells in mice. *Diabetes*, **62**, 2762-2772.

95. Ordway, D., Henao-Tamayo, M., Harton, M., Palanisamy, G., Troudt, J., Shanley, C., Basaraba, R.J., and Orme, I.M. (2007) The hypervirulent *Mycobacterium tuberculosis* strain HN878 induces a potent TH1 response followed by rapid down-regulation. *J Immunol*, **179**, 522-531.

96. Noble, A., Giorgini, A., and Leggat, J.A. (2006) Cytokine-induced IL-10-secreting CD8 T cells represent a phenotypically distinct suppressor T-cell lineage. *Blood*, **107**, 4475-4483.

97. Sun, J., Madan, R., Karp, C.L., and Braciale, T.J. (2009) Effector T cells control lung inflammation during acute influenza virus infection by producing IL-10. *Nat Med*, **15**, 277-284.

98. Flores-Garcia, Y., Rosales-Encina, J.L., Satoskar, A.R., and Talamas-Rohana, P. (2011) IL-10-IFN-gamma double producers CD4+ T cells are induced by immunization with an amastigote stage specific derived recombinant protein of *Trypanosoma cruzi. Int J Biol Sci*, **7**, 1093-1100.

99. Jankovic, D., Kullberg, M.C., Feng, C.G., Goldszmid, R.S., Collazo, C.M., Wilson, M., Wynn, T.A., Kamanaka, M., Flavell, R.A., and Sher, A. (2007) Conventional T-bet(+)Foxp3(-) Th1 cells are the major source of host-protective regulatory IL-10 during intracellular protozoan infection. *J Exp Med*, **204**, 273-283.

100. Chen, J. and Liu, X.S. (2009) Development and function of IL-10 IFN-gamma-secreting CD4(+) T cells. *J Leukoc Biol*, **86**, 1305-1310.

101. Roffe, E., Rothfuchs, A.G., Santiago, H.C., Marino, A.P., Ribeiro-Gomes, F.L., Eckhaus, M., Antonelli, L.R., and Murphy, P.M. (2012) IL-10 limits parasite burden and protects against fatal myocarditis in a mouse model of *Trypanosoma cruzi* infection. *J Immunol*, **188**, 649-660.

102. Cohen, C.A., Shea, A.A., Heffron, C.L., Schmelz, E.M., and Roberts, P.C. (2013) Intra-abdominal fat depots represent distinct immunomodulatory microenvironments: a murine model. *PLoS One*, **8**, e66477.